From THE DEPARTMENT OF PHYSIOLOGY AND PHARMACOLOGY

Karolinska Institutet, Stockholm, Sweden

BRIDGING IMMUNE ACTIVATION WITH THE KYNURENINE PATHWAY - IMPLICATIONS FOR PSYCHOSIS

Markus Larsson

Karolinska Institutet

Stockholm 2015

Published by Karolinska Institutet.
Printed by US-AB

ISBN 978-91-7549-977-2

Bridging immune activation with the kynurenine pathway - implications for psychosis

THESIS FOR DOCTORAL DEGREE (Ph.D.)

By

Markus Larsson

Principal Supervisor:
Associate Professor Sophie Erhardt
Karolinska Institutet
Department of Physiology and Pharmacology

Co-supervisor:
Dr. Lilly Schwieler
Karolinska Institutet
Department of Physiology and Pharmacology

Opponent:
Assistant Professor Jason O'Connor
University of Texas
Department of Pharmacology

Examination Board:
Associate Professor Tomas Deierborg
Lund University
Department of Experimental Medical Science

Associate Professor David Engblom
Linköping University
Department of Clinical and Experimental Medicine

Associate Professor Jan Kehr
Karolinska Institutet
Department of Physiology and Pharmacology

ABSTRACT

Kynurenic acid (KYNA), an endogenous *N*-Methyl-D-aspartic acid receptor (NMDAR) antagonist, is elevated in patients with schizophrenia. In addition, elevated levels of KYNA are associated with activation of the immune system, which also has been implicated in the development and maintenance of psychotic disorders, including schizophrenia.

The aim of this thesis was to further investigate the role of KYNA in the pathophysiology of schizophrenia. Thus, patients with schizophrenia were examined with respect to cerebrospinal fluid (CSF) levels of interleukin (IL)-6, kynurenines, and the functional effects of G protein-coupled receptor kinase 3 (GRK3) expression. Mice administered lipopolysaccharide (LPS), amphetamine, or lacking the immune-regulating enzyme GRK3, were studied with respect to biochemical and functional aberrations associated with schizophrenia.

The elevated CSF levels of IL-6 found in patients with schizophrenia were associated with increased CSF KYNA levels. Administration of IL-6 increased KYNA production in astrocytes and lower GRK3 expression in healthy individuals correlated to increased CSF KYNA levels. GRK3 was further found to be associated with psychosis in patients with bipolar disorder.

Subchronic elevation of KYNA, or lack of GRK3 augmented the amphetamine response as verified by increased locomotor activity and dopamine release. Signs of amplified immune activity were evident in *Grk3*$^{-/-}$ mice by increases in astrocyte markers, IL-1β, kynurenine, and KYNA turnover. Intracerebroventricular (ICV) administration of IL-1β, and dual, bot not single injections of LPS increased brain KYNA. In addition, mice injected ICV with IL-1β or lacking GRK3 showed disrupted prepulse inhibition (PPI).

Results presented here point to an intimate relationship between immune activation, the kynurenine pathway, and psychosis. Specifically, immune activation, present in patients with schizophrenia, was demonstrated to activate the kynurenine pathway. In addition, activation of the kynurenine pathway induced KYNA and lead to behavioral aberrations in rodents.

LIST OF SCIENTIFIC PAPERS

I. Olsson, S. K., **Larsson, M. K**., Erhardt, S. (2012). Subchronic elevation of brain kynurenic acid augments amphetamine-induced locomotor response in mice. *Journal of Neural Transmission (Vienna, Austria : 1996)*, *119*(2), 155–163. doi:10.1007/s00702-011-0706-6

II. Schwieler, L*., **Larsson, M. K***., Skogh, E., Kegel, M. E., Orhan, F., Abdelmoaty, S., et al. (2014). Increased levels of IL-6 in the cerebrospinal fluid of patients with chronic schizophrenia - significance for activation of the kynurenine pathway. *Journal of Psychiatry & Neuroscience : JPN*, *39*(6), 140126. doi:10.1503/jpn.140126
*These authors contributed equally to this work

III. Carl Sellgren*, **Markus Larsson***, Funda Orhan, Magdalena E Kegel, Ida Nilsson, Susan B Powell, S Caldwell, M Kamenski, Sarah E Bergen, Lilly Schwieler, Camilla I Svensson, Paul Lichtenstein, Martin Schalling, Mikael Landén, Göran Engberg, Sophie Erhardt. *Targeting of GRK-3 identifies a molecular pathway leading to glial activation in psychotic disorders*. Manuscript
* These authors contributed equally to this work.

IV. **Larsson, M.K**, Faka A, Bhat M, Goiny M, Orhan F, Oliveros A, Ståhl S, Liu XC, Choi DS, Sandberg K, Engberg G, Schwieler L, Erhardt S. (2015) *Repeated LPS injections induce disparate changes in the kynurenine pathway versus a single injection - Relevance for animal models of psychiatric disorders.* Manuscript

CONTENTS

LIST OF ABBREVIATIONS

3-HK	3-Hydroxykynurenine
5-HIAA	5-Hydroxyindoleacetic acid
5-HT	5-Hydroxytryptamine (Serotonin)
aCSF	Artificial cerebrospinal fluid
ANOVA	Analysis of variance
ATP	Adenosine triphosphate
AUC	Area under curve
BPRS	Brief Psychiatric Rating Scale
CNS	Central nervous system
COX	Cyclooxygenase
CSF	Cerebrospinal fluid
DOPAC	3,4-Dihydroxyphenylacetic acid
e.g.	For example (exempli gratia lat.)
EDTA	Ethylenediaminetetraacetic acid
EGTA	ethylene glycol tetraacetic acid
GAF	Global assessment of functioning
GFAP	Glial fibrillary acidic protein
GRK3	G-protein coupled kinase 3
GWAS	Genome-wide association study
HPLC	High-performance liquid chromatography
HVA	Homovanillic acid
i.p.	Intraperitoneal
IC_{50}	half maximal inhibitory concentration
ICV	Intracerebroventricular
IDO	Indoleamine 2,3-dioxygenase
IFN	Interferon

IL	Interleukin
KAT	Kynurenine aminotransferase
KMO	Kynurenine monooxygenase
KO	Knock-out
KYNA	Kynurenic acid
LA	Locomotor activity
LPS	Lipopolysaccaride
NFκB	Nuclear factor kappa B
NMDAR	N-Methyl-D-aspartic acid receptor
P2X7	P2X purinoceptor 7
PCA	Perchloric acid
PCP	Phencyclidine (Angel dust)
PFA	Paraformaldehyde
PPI	Prepulse inhibition
QUIN	Quinolinic acid
s.c.	Subcutaneous
SNP	Single nucleotide polymorphism
TDO	Tryptophan 2,3-dioxygenase
TLR	Toll-like receptor
α7nAChR	α7 nicotinic acetylcholine receptor

1 INTRODUCTION

Hypotheses regarding the immune system as a contributor to the development of psychiatric disorders have been put forward since the early 1900s. However, these were at large rejected as the central nervous system (CNS) was believed to be an immune-privileged area. Clinical observations and experiments have since then dramatically changed our view of the interaction between the brain and the immune system. These findings have without a doubt been of great importance for our understanding of the human brain and may hopefully lead to more effective treatments for psychiatric disorders.

1.1 SCHIZOPHRENIA

The disorder later coined as schizophrenia by Eugene Bleuler (Bleuler, 1911) was first described by the german psychiatrist Emil Kraepelin in the end of the nineteenth century (Kraepelin, 1896). Patients that suffer from schizophrenia experience a wide range of symptoms that distort their sense of reality. In addition and perhaps not as recognized is the excess mortality (Saha et al., 2007), including death by suicide that follows the disorder.

Current studies estimate the point prevalence of schizophrenia at approximately 0.5 % (McGrath et al., 2008). Schizophrenia has a massive socioeconomic impact (estimated annual cost in US ~ $23 billion (Desai et al., 2013)), and causes an immense suffering for affected individuals and their relatives. Prior to the onset of the disorder, a prodromal syndrome exists when symptoms such as withdrawal, depression, and paranoia may present (Yung and McGorry, 1996). Efforts are currently being put into identifying individuals with a high risk of developing full-blown schizophrenia as some studies indicate that treatment may delay or prevent transition to psychosis (Stafford et al., 2013). The risk of developing schizophrenia peaks in late teens, after the mid-twenties the risk declines substantially while there is a slight increase in the incidence again in menopausal women (Gupta et al., 2012).

The symptoms of schizophrenia are classified into three clusters: **i**) *positive symptoms*, which entail symptoms that are present in the patient population, but not in healthy individuals. These symptoms include hallucinations and delusions. **ii**) *negative symptoms* refer to personality traits absent in afflicted individuals that used to be present prior to disease onset, and are also present in healthy individuals. These symptoms usually include anhedonia, loss of social interest, blunted affect, and lack of motivation. **iii**) *cognitive symptoms* refer to disturbances in thought processes and include but are not limited to: working and long-term memory problems and attention deficits. See Andreasen and Olsen, 1982 for overview of the classification system.

Patients are usually treated with antipsychotic drugs. These were discovered in the 1950s and were later shown to exert their effect by blocking dopamine receptors. The contemporary arsenal of antipsychotic drugs quite effectively ameliorates the positive symptoms of schizophrenia.

However, there is still a large unmet need in the treatment of negative and cognitive symptoms, and it is these symptoms that to a large degree determine the level of functioning in patients (Tamminga et al., 1998).

Several factors that increase the risk of developing schizophrenia have been identified. The strongest is family history, suggesting a major genetic influence. In support of this, it has been estimated that around 80% of the risk of developing schizophrenia is explained by genetic factors (Cannon et al., 1998; Cardno et al., 1999; Sullivan et al., 2003). Additional evidence of strong genetic influence is provided by twin adoption studies showing concordance rates around 50 % (Cardno and Gottesman, 2000). It has further been shown that there is a substantial overlap between risk genes for schizophrenia and bipolar disorder. Other identified risk factors include migration, male sex, urban living (McGrath et al., 2004), and heavy adolescent marijuana use (Semple et al., 2005). The prevalence, however, seems to be equal among non-developed and developed countries (Mellergard, 1980).

1.2 IMMUNOLOGICAL ASPECTS

Early evidence of immune involvement in schizophrenia comes from observations of an increase in the incidence of psychosis in areas affected by the influenza pandemic in 1918 (Menninger, 1919). Prior to the introduction of antipsychotic drugs, patients with schizophrenia received pyro therapy (fever induction), however with mixed results as some patients deteriorated again after treatment (Jauregg, 1926). More recent studies show that birth in late winter may be a risk factor for later development of schizophrenia, possibly due to viral infections (Baron and Gruen, 1988). Moreover, offspring to mothers exposed to infectious agents (e.g. toxoplasma gondii, influenza, herpes virus) during pregnancy have an increased risk of developing psychotic disorders, including schizophrenia (Yolken and Torrey, 2008). Interestingly, offspring's risk of developing schizophrenia in adulthood has been associated with increased maternal levels of the pro-inflammatory cytokine interleukin (IL)-8, regardless of the reason for this elevation (Brown et al., 2004). This points to maternal immune activation as the culprit that renders offspring vulnerable and not the infectious agent per se. No single immunological factor has yet been identified that fully explains the wide range of symptoms and pathology of schizophrenia. However, large genome-wide association studies (GWAS) have identified regions containing immune-related genes as significantly associated with schizophrenia (Shi et al., 2009). Clinical studies point to distinctive patterns of immune activation during different stages of the disorder (Miller et al., 2011). For instance, the cytokine IL-1β is increased in the cerebrospinal fluid (CSF) of patients with a recent onset of the disorder (Söderlund et al., 2009). As immune cells coordinate the immune response by the release of cytokines, increased levels of cytokines may thus indicate increased immune activity in these patients.

1.2.1 The main glial cells in the nervous system

Previously seen as merely providing a scaffold for neurons, astrocytes have in recent years been recognized as important contributors to brain function. Astrocytes may reside in proximity to synapses, where they perform multiple duties such as neurotransmitter recycling, metabolic support, and regulation of ion concentrations in the extracellular space (Walz, 2000). The major influence of astrocytes on synaptic neurotransmission has widened the synapse concept into a tripartite synapse model (Araque et al., 1999).

Microglial cells are predominantly viewed as the resident macrophages of the CNS. They are derived from a distinct monocytic lineage that migrate to the brain neonatally. During adulthood, microglia continuously scan their immediate microenvironment for signs of tissue damage and infection (Nimmerjahn et al., 2005). This state is often referred to as a "resting", or quiescent state. However, upon activation by antigen or inflammatory mediators, microglia transform to an active state. Activated microglia express a wide range of immune-related genes, including pro-inflammatory cytokines and major histocompatibility complex (MHC) class I/II, thereby capable of initiating and maintaining inflammation. Studies indicate increased microglial activation in patients as verified by imaging studies (Doorduin et al., 2009; van Berckel et al., 2008).

In light of the increased support for immune disturbances in patients, and the relative lack of effect on the negative and cognitive symptoms by standard antipsychotic drugs, attention has turned to treatment options that target the immune system. Interestingly, the antimicrobial agent minocycline that inhibits microglial activation decrease negative symptoms in patients when added to antipsychotic drugs (Levkovitz et al., 2010; F. Liu et al., 2014). Similarly, cyclooxygenase (COX)-2 inhibitors have been shown to improve cognitive symptoms as an add-on treatment (Müller et al., 2005). Treatment with COX-2 inhibitors in rats decreases brain levels of kynurenic acid (KYNA), which is detrimental to cognition (see 1.4; Animal models). It might, therefore, be speculated that the improved cognition are due to decreased levels of KYNA.

1.2.2 The P2X7 receptor

Purinergic signaling is a key immune regulatory mechanism. The P2 receptor family receives input from nucleotides and is further divided into P2Y and P2X receptors. P2Y receptors are G protein-coupled receptors (GPCRs) while P2X receptors, including P2X purinoceptor 7 (P2X7) are ion channels (Eltzschig et al., 2012; Jiang et al., 2013). P2X7 receptors are expressed by several cell types in the CNS, including astrocytes and microglia. The endogenous ligand of P2X7 is adenosine triphosphate (ATP), an abundant molecule that in addition to its energy carrying properties increases in tissues following events such as tissue damage and infection. In addition, ATP participates in glia-neuron signaling and modulates synaptic transmission (Fields and Burnstock, 2006). Activation of P2X7 induces channel opening, allowing K^+ efflux from the cell. Although not fully clarified, the change in the $[K^+]$ gradient is believed to induce the opening

of pannexin channels, which in turn via downstream signaling events, leads to the assembly of the inflammasome complex (Sperlágh and Illes, 2014). Caspase-1 is the critical component of the inflammasome in terms of IL-1β activation, as it cleaves pro-IL-1β into its active form (Martinon et al., 2007; Minkiewicz et al., 2013; Sanz and Di Virgilio, 2000).

1.2.3 G-protein coupled receptor kinase 3

G-protein coupled receptor kinase (GRK) 3, also known as ADRBK2, belongs to a ubiquitous family of kinases that primarily phosphorylates GPCRs and consequently inhibits their activity. Importantly, GRK3 phosphorylates P2X7 receptors (Feng et al., 2005), inhibiting further downstream signaling to caspase-1. Loss-of function of GRK3 may thus cause P2X7 receptor overactivation, leading to excess IL-1β release (**Figure 1**). In line with the hypothesis of increased immune activation in psychiatric disorders, reduced expression of GRK3 has been found in the dorsolateral prefrontal cortex of patients with schizophrenia (Bychkov et al., 2011) and bipolar disorder (Rao et al., 2009; Shaltiel et al., 2006)

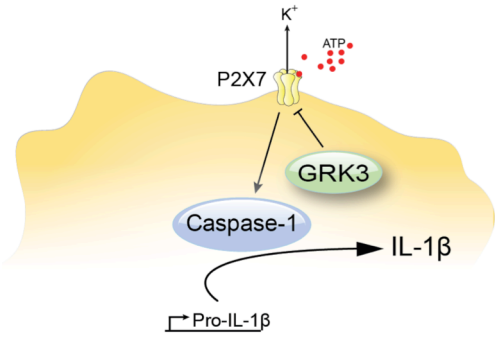

Figure 1. GRK3 dependent phosphorylation of P2X7 in astrocytes or microglia.

1.3 KYNURENIC ACID AND SCHIZOPHRENIA

Several lines of evidence point to dysregulation of the kynurenine pathway in schizophrenia. For instance, patients with schizophrenia display increased levels of KYNA in the CSF and post mortem brain (Erhardt et al., 2001a; Linderholm et al., 2012; Nilsson et al., 2005; Schwarcz et al., 2001). Further, studies show increased KYNA and decreased kynurenine monooxygenase (KMO) activity in post-mortem brain tissue from patients with schizophrenia (Sathyasaikumar et al., 2011; Wonodi et al., 2011).

The first member of the kynurenine pathway described was KYNA, extracted from dog urine in 1853 by Justus Von Liebig (Liebig, 1853). Over a decade later, KYNA was found to be present in the human brain (Moroni et al., 1988). Pharmacodynamically, KYNA acts as a non-competitive antagonist at the glycine site of the *N*-Methyl-D-aspartic acid receptor (NMDAR, $IC_{50} \approx 8 – 15$ μM). At higher concentrations it also blocks the glutamate recognition site of the NMDAR ($IC_{50} \approx 0.2 – 0.5$ mM), and also the glutamate receptors of the α-amino-3-hydroxy-5-methyl-4-isoxazolepropionic acid (AMPA) and kainate type (IC_{50} in the millimolar range). Further, KYNA competitively blocks the α7 subunit containing nicotinic acetylcholine receptor (α7nAChR, $IC_{50} \approx 7$ μM, Hilmas et al., 2001). KYNA has also been shown to interact with the previous orphan receptor GPR35 (Wang et al., 2006), and the aryl hydrocarbon receptor

(DiNatale et al., 2010), although the physiological significance of these interactions have yet to be fully determined.

1.3.1 The kynurenine pathway

The majority of available tryptophan is broken down by the kynurenine pathway as opposed to 5-hydroxytryptamine (5-HT, Serotonin) formation (Gál and Sherman, 1980).The initiation of tryptophan breakdown by the kynurenine pathway (**Figure 2**) is the oxidation of tryptophan into *N*-formyl-kynurenine by the rate-limiting enzymes of the kynurenine pathway, indoleamine 2,3-dioxygenase (IDO) and/or tryptophan 2,3-dioxygenase (TDO). *N*-formyl-kynurenine is then transformed to kynurenine, the central component of the pathway, by kynurenine formamidase. As kynurenine readily passes the blood-brain barrier (BBB), about 60% of the central pool of kynurenine is of peripheral origin (Gál and Sherman, 1980). From this point on, the pathway is spatially separated as kynurenine may be converted into KYNA by astrocytic kynurenine aminotransferases (KATs) I/II/III/IV, or into 3-hydroxykynurenine (3-HK) by microglial KMO. 3-HK is then further metabolized into quinolinic acid (QUIN), which as opposed to KYNA is an agonist at the NMDAR with excitotoxic and seizurogenic properties (Lapin, 1978; Stone and Perkins, 1981). In fact, local QUIN administration into the brain has even been shown to induce lesions (Schwarcz et al., 1983).

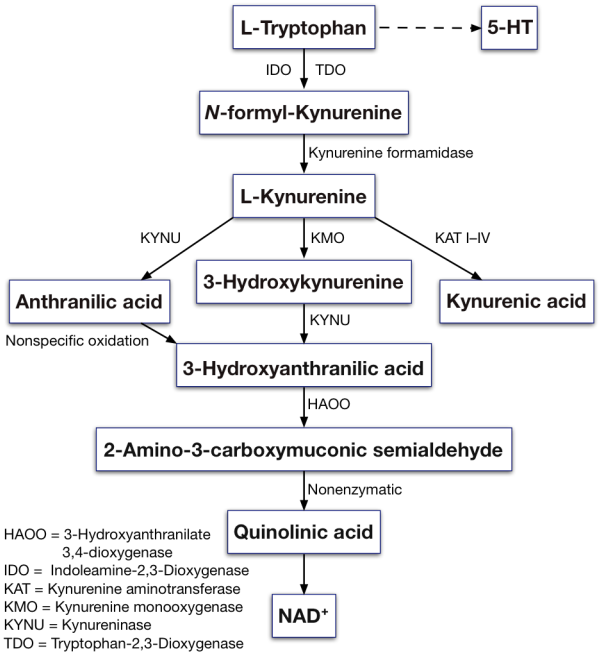

Figure 2. The kynurenine pathway of tryptophan breakdown.

1.3.2 Regulation of the kynurenine pathway

The immune system exerts a strong influence on the kynurenine pathway. Upon immune activation, the release of pro-inflammatory cytokines such as IL-1β, IL-6, and interferon (IFN)-γ causes activation of the kynurenine pathway primarily through their action on IDO/TDO, see Campbell et al., 2014. Activation of the kynurenine pathway decreases available tryptophan, and it has been speculated that this might serve as a crude antibacterial mechanism, as tryptophan is essential to growing microbes (Zelante et al., 2009). The limiting factor in KYNA synthesis is the availability of kynurenine. The administration of kynurenine (Swartz et al., 1990) or KMO inhibitors (Moroni et al., 2005) therefore consistently increase KYNA in the CNS. Additionally, administration of probenecid, which blocks CNS KYNA efflux by the human organic anion transporters (hOATs), also reliably increases brain levels of KYNA (Uwai et al., 2012).

1.4 ANIMAL MODELS OF SCHIZOPHRENIA

Animal models of psychiatric disorders are valuable tools in research as they enable the controlled investigation of functional effects of suggested pathophysiological mechanisms. As psychiatric disorders display a plethora of symptoms, only particular traits are usually successfully modeled. Further, these traits may not be exclusive to a single disorder. For instance, anhedonia is a symptom usually present in both depression and schizophrenia that renders the affected individual unable to experience pleasure. This may be modeled in animals by measuring the absence of the hedonistic drive of drinking sweetened water. Animal models of schizophrenia may be broadly classified as developmental, genetic, lesional and pharmacological. These categories are however not mutually exclusive.

Various types of behavioral assessments are usually performed in validating phenotypes, one such is prepulse inhibition (PPI) of the acoustic startle reflex. Here, the startle response to a short intense auditory stimulus (pulse) is measured with and without a preceding non-startling auditory short stimulus (prepulse). Failure by the prepulse to inhibit the startle response reflects deficits in sensorimotor gating, a common finding among patients with schizophrenia (Braff et al., 1978; Swerdlow et al., 2008). Such gating deficits have been suggested to reflect problems with filtering out irrelevant auditory stimuli, and intrusive thoughts (McGhie and Chapman, 1961). Moreover, PPI deficits can be induced in animals by various means, e.g. psychotomimetic drugs (Geyer et al., 2001), or targeted gene deletions (Powell et al., 2009), and rescued by administration of atypical antipsychotic drugs (Fijał et al., 2014; Li et al., 2011).

Increased spontaneous and drug-induced hyperlocomotion may reflect abnormalities in dopaminergic transmission and are commonly tested in rodents. Further, there is an interaction between KYNA and the dopamine system, as elevation of KYNA potentiates amphetamine-induced dopamine release (Olsson et al., 2009), and increases the firing activity of midbrain dopaminergic neurons (Erhardt et al., 2001b; Linderholm et al., 2007).

1.4.1 Developmental, genetic, and lesion models

Developmental animal models entail insults to central developmental processes for example using NMDAR antagonists during the prenatal, perinatal or postnatal period. These insults may interfere with neuronal guiding (Reiprich, 2004), leading to behavioral disturbances in adulthood (Lim et al., 2012; Muraki and Tanigaki, 2015). In analogy with this, neonatal kynurenine treatment and influenza virus infection, both cause transient elevation of KYNA and induce behavioral aberrations in adult mice (X. C. Liu et al., 2014).

Genetic models commonly involve the creation of knock-out (KO) mice by deletion of the gene of interest in mice, thus enabling the study of the phenotypic contribution of a single gene. Schizophrenia-like phenotypes have successfully been created by the deletion of suggested risk genes for schizophrenia. For instance, mice with deletion of "disrupted in schizophrenia-1" (DISC1), a gene associated with schizophrenia, display deficits in several behavioral parameters (Lipina and Roder, 2014). Deletions of genes related to immune function have also been reported to cause functional disturbances. In one study, virus infection caused deficits in sensorimotor gating in KO mice lacking the "transporter associated with antigen processing 1" (TAP1) gene, but not in wild-type mice (Asp et al., 2010). TAP1 KO mice lack functional $CD8^+$ T-cells, resulting in increased activity of the innate immune (Asp et al., 2009). As described previously (see 1.3.1; The kynurenine pathway), KAT II converts kynurenine into KYNA. Notably, inactivation of KAT II by deletion (KO mice) or pharmacological blockade in rats and nonhuman primates improves cognitive function (Kozak et al., 2014; Potter et al., 2010), whereas there is a cognitive disrupting effect by increased KYNA (Alexander et al., 2012).

Lesional models may entail permanent inactivation of brain areas with neurotoxic substances such as 6-hydroxydopamine, see Lipska and Weinberger, 2002. This model has however been criticized for it lack of construct validity. Interestingly, a transient lesion model has been developed where animals develop a similar phenotype as in the permanent model. Here, transient inactivation of the ventral hippocampus by postnatal tetrodotoxin administration causes cognitive deficits which are reversed by treatment with an α7nAChR agonist (Brooks et al., 2012).

1.4.2 Immune models

Induction of the immune system in humans and rodents induces a coordinated repertoire of behaviors termed "sickness behavior". It has been suggested that this is a behavioral adaption induced by the immune system during infection to increase chances of survival, see Hart, 1988. In rodents, sickness behavior can reliably be induced by lipopolysaccharide (LPS), a component of the outer membrane of gram-negative bacteria (Dunn and Swiergiel, 2005). LPS is recognized by toll-like receptor (TLR) 4, which is present primarily on microglia and astrocytes in the CNS (Dong and Benveniste, 2001; Falsig et al., 2008). Activation of TLR4 induces a down-stream cascade that enables nuclear factor kappa B (NFκB) mediated transcription of pro-IL-1β and pro-

IL-18 (Rhee and Hwang, 2000). This induces in addition to social withdrawal, decreased appetite, and fatigue, also symptoms congruent with certain aspects of the human state of schizophrenia and depression, such as anhedonia (Salazar et al., 2012; Walker et al., 2013) and cognitive deficits (Czerniawski et al., 2015; Haba et al., 2012; Ming et al., 2015). The behavioral aberrations in LPS treated rodents are likely mediated by activation of the kynurenine pathway as IDO inhibition ameliorates depressive-like symptoms, but not sickness per se (O'Connor et al., 2009).

1.5 THE DOPAMINE AND GLUTAMATE HYPOTHESIS OF SCHIZOPHRENIA

The impact of the dopamine system on the development and maintenance of psychosis is based on observations that enhancers of dopaminergic transmission such as amphetamine, exacerbate psychotic symptoms, while antagonists, such as antipsychotic drugs, ameliorate them (Carlsson et al., 2001; Sanfilipo et al., 1996; Snyder, 1973). Corroborating evidence has been provided in contemporary studies where the dopaminergic hyperresponsiveness following amphetamine is demonstrated in patients (Abi-Dargham et al., 1998; Abi-Dargham and Laruelle, 2005; Abi-Dargham et al., 2000; Breier et al., 1997b; Laruelle et al., 1996). These findings form the basis of the dopamine hypothesis of schizophrenia. This hypothesis has however been revised as it poorly accounts for the negative and cognitive symptoms. The modified dopamine hypothesis, thus suggests that decreased dopaminergic transmission in prefrontal brain areas coexist with a midbrain hyperdopaminergic state (Davis et al., 1991) is now generally accepted.

Aberrations in glutamatergic transmission have also been implicated in the pathophysiology of schizophrenia as low CSF glutamate levels in patients have been reported (Kim et al., 1980). In addition, NMDAR antagonists (e.g. ketamine, MK-801, and phencyclidine) aggravate psychotic symptoms in patients with schizophrenia (Lahti et al., 2001), and have been shown to induce psychotic symptoms from all spectra (Krystal et al., 2005) in healthy individuals (Allen and Young, 1978; Breier et al., 1997a). Interestingly, studies show that NMDAR antagonist-induced PPI deficits respond poorly to classical antipsychotics (Bakshi et al., 1994), while treatment with the atypical antipsychotic clozapine treatment reverses such PPI deficits and protects against ketamine induced psychosis (Malhotra et al., 1997).

2 AIMS

- To study the influence of elevated brain KYNA on dopaminergic neurotransmission by studying the effect of kynurenine administration on amphetamine-induced hyperlocomotion in mice.

- To measure CSF cytokines in patients with chronic schizophrenia and correlate to previously measured kynurenines from the same patients.

- To investigate the effects of IL-6 administration on KYNA production in human fetal astrocytes.

- To investigate biochemical aberrations and behavior in *Grk3* mutant mice.

- To study the importance of GRK3 on CSF KYNA levels and psychosis in patients with bipolar disorder.

- To investigate the effect of dual versus single administration of LPS with respect to brain and serum kynurenines.

3 MATERIALS AND METHODS

The following sections are brief descriptions of the materials and methods used. For details see the corresponding section in respective paper.

3.1 DRUGS AND CHEMICALS (PAPERS I – IV)

Compound	Compound
$^{13}C_3{}^{15}N_1$-QUIN[6]	Lipopolysaccharide (LPS)[1]
5-Hydroxytryptamine (5-HT)[1]	Methanol[1]
Acetic acid[1]	NaCl[1]
Acetonitrile[1]	NaOH[1]
Acrylic dental cement (Dentalon®)[3]	Octanesulfonic Acid[1]
Anti P2X7 Receptor antibody (APR-004)[4]	Perchloric Acid (PCA)[1]
Anti β-Actin antibody	Paraformaldehyde (PFA)[1]
Bupivacaine (Marcain®)[2]	Phosphatase Inhibitor Cocktail I (P2850)[1]
D-Amphetamine[1]	Phosphatase Inhibitor Cocktail II (P5726)[1]
D_4-5-HT[1]	Phosphatase Inhibitor Cocktail III (P0044)[1]
D_4-Kynurenine (D_4-KYN)[7]	Phosphate buffered saline (PBS)[1]
D_5-Tryptophan (D_5-TRP)[1]	Probenecid[1]
Ethylene glycol tetraacetic acid (EGTA)[1]	Protease Inhibitor Cocktail (P8340)[1]
Ethylenediaminetetraacetic Acid (EDTA)[1]	Protease Inhibitor Cocktail (11836170001)[8]
Formic Acid[1]	Sodium Acetate[1]
GFAP antiserum[1]	Sodium Dodecyl Sulphate[1]
Horseradhish Peroxidase Conjugated Secondary Antibodies (7076, 7074)	Sodium Metabisulfite[1]
Interferon (IFN)-γ[1]	Tris-HCl pH 7.5[1]
Interleukin (IL)-1β, mouse[1]	Triton X-100[1]
Isoflurane (Furane®)[2]	Tryptophan (TRP)[1]
Kynurenic acid (KYNA)[1]	Tween 20[1]
L-Kynurenine[1]	Zinc Acetate[1]

Table 1. Drugs and chemicals. Suppliers: 1. Sigma-Aldrich, Stockholm, Sweden 2. Astra Zeneca, Södertälje, Sweden 3. Heraeus, Hanau, Germany 4. Alomone Labs, Jerusalem, Israel 5. Cell signaling Technology, Danvers, MA, USA 6. Synfine Research Inc., Ontario, Canada 7. Buchem B.V., Apeldoorn, The Netherlands 8. Roche Diagnostics Corporation, Indianapolis, IN, USA

See **Table 1** for manufacturer details. For **paper I**, kynurenine was dissolved in sterile dH_2O and pH was thereafter adjusted to ≈ 8.5 with NaOH. D-Amphetamine (**paper I, III**) and probenecid (**paper III**) were dissolved in sterile dH_2O. LPS (Escherichia coli 0111:B4**)** in **paper IV** was dissolved in sterile saline. IL-1β (**paper III**) was dissolved in sterile dH_2O to a concentration of 0.1 mg/ml and further diluted with phosphate buffered saline (PBS).

The lysis buffer in **paper III** contained 150 mM NaCl, 20 mM Tris pH 7.5, 1 mM ethylenediaminetetraacetic acid (EDTA), 1mM ethylene glycol tetraacetic acid (EGTA), 1 % triton X-100. The complete hypotonic buffer in **paper III** was prepared by adding 10 µl $NaHCO_3$ (1 M) to 9 990 µl dH_2O, to which phosphatase inhibitor cocktail I (1:1 000), II (1:1 000), and protease inhibitor cocktail (P8340, 1:1 000) were added. Complete extraction buffer was composed of 0.50 % Triton X-100, 50 mM Tris-HCl (pH 7.5), 150 mM NaCl, 1 mM EDTA, 1 % sodium dodecyl sulfate, protease inhibitor cocktail, phosphatase inhibitor cocktail I, II. Tris buffer for western blotting was composed of 50 mM Tris-HCl, 6 mM NaCl, and 0.1 % Tween 20. The anti P2X7 receptor and anti β-actin antibodies were diluted 1:10 000.

For immunohistochemistry experiments in **paper III**, the following solutions were used: 4 % para-formaldehyde (PFA) containing 0.4 % picric acid in 0.16 M phosphate buffer (pH 6.9), TNT buffer (0.1 M Tris-HCl (pH 7.5), 0.15 M NaCl, 0.05 % Tween 20), TNB buffer (0.1 M Tris-HCl (pH 7.5), 0.15 M NaCl, 0.5 % blocking reagent). The anti-rabbit horseradish-peroxidase conjugated secondary antibody was diluted in TNB buffer for 30 min (1:200). The Biotinyl tyramide fluorescein conjugate was diluted 1:1 200 in amplification diluent.

Artificial CSF (aCSF, **paper III**) contained 148 mM NaCl, 4 mM KCl, 0.8 mM $MgCl_2$, 1.4 mM $CaCl_2$ in dH_2O. The mobile phase (**papers I – IV**) for detection of brain/serum KYNA and serum kynurenine was 50 mM sodium acetate in ultra-pure dH_20 (adjusted to pH 6.2 with acetic acid) with 7 % acetonitrile. The mobile phase composition for electrochemical detection of brain tissue dopamine, 5-HT, 5-Hydroxyindoleacetic acid (5-HIAA), homovanillic acid (HVA), and 3,4-Dihydroxyphenylacetic acid (DOPAC) in **paper IV** was (concentrations used in **paper III** for microdialysate analysis are in parenthesis): 70 (55) mM sodium acetate, 1.5 (1.16) mM octanesulfonic acid, 0.01 mM EDTA, 20 (10) % Methanol, in dH_2O. pH was adjusted to 4.1 with acetic acid. The perchloric acid (PCA) solution for tissue homogenization was composed of 70% PCA diluted to 0.4 M in dH_20, containing 0.1 % sodium metabisulfite and 0.05 % EDTA.

3.2 ASTROCYTE CULTURES (PAPER II)

Human embryonic primary cortical astrocytes (ScienCell™ Research Laboratories, Carlsbad, CA USA) in passage four were starved for 24 h (0.02 % fetal bovine serum, 0.01 % growth supplement mix). Next, 10 ng/ml IL-6 was applied and supernatants were collected after 24, 48, and 72 h, and immediately put on dry ice and stored at -80 °C until analysis. Cells were cultured according to manufacturers protocols and experiments were performed in triplicates, repeated twice.

3.3 P2X7 INTERNALIZATION (PAPER III)

3.3.1 Separation of membrane fractions

Mice brain tissue was homogenized in complete hypotonic buffer and then centrifuged for 10 min 4 °C (1 200 × g). The supernatant was centrifuged (21 600 × g, 4 °C, 30 min), and the resulting internal membrane-containing pellet (P2) was resuspended in complete extraction buffer. The supernatant was centrifuged at 150 000 × g for 2 h at 4 °C and the plasma membrane-containing pellet (P3) was dissolved in complete extraction buffer. P3 was then washed with complete hypotonic buffer and centrifuged for 2 h at 150 000 × g (4 °C). This pellet was resuspended in complete extraction buffer. A Pierce™ BCA protein assay kit (Thermo Fisher Scientific Inc., Waltham, MA, USA) was used for protein content determination according to manufacturers recommendation.

3.3.2 Western blot

P2 and P3 containing fractions were separated on a NuPAGE 4 – 12 % Bis-Tris gel (Invitrogen, Carlsbad, CA, USA) before being transferred to nitrocellulose membranes (Invitrogen). The membranes were then blocked with reconstituted dried milk (5 % in Tris buffer) for 1 h at room temperature. Next, membranes were incubated with a primary antibody against P2X7 overnight at 4 °C. Following three washes (5 min each), membranes were incubated with horseradish peroxidase conjugated secondary antibodies at room temperature for 1 h. Chemiluminescent detection reagents (Supersignal™ West Pico, West Femto, Thermo Fisher Scientific Inc.) were used to visualize specific bands. An anti β-actin antibody was used as protein loading control to which the P2X7 signals were normalized. The Quantity One software (Bio-Rad Laboratories, Hercules, CA, USA) was used for signal intensity measurements.

3.4 IMMUNOHISTOCHEMISTRY (PAPER III)

Mice were anesthetized with pentobarbital (50 mg/kg) and perfused via the ascending aorta with 37 °C Tyrode's solution (Ca^{2+} free) followed by 37 °C, 4 % PFA. Next, mice were perfused with 4 °C, 4 % PFA and decapitated. Brain were harvested and immersed in ice-cold PFA for 90 min and rinsed overnight in phosphate-buffered 10 % sucrose, set to pH 7.4. Before being thaw-mounted (Superfrost® slides, WVR International, Radnor, PA, USA) brains were CO_2 frozen and cut in 14 μm sections in a cryostat (Microm, Heidelberg, Germany). Sections spanning around he bregma (0.98-(-2.30)) were included in the analysis and were pretreated with 0.03 % H_2O_2 and incubated with glial fibrillary acidic protein (GFAP) antiserum overnight 4 °C. Brain sections were then processed according to the TSA-plus Fluorescein System (PerkinElmer, Waltham, MA, USA). In short, sections were washed in TNT buffer and then incubated in TNB buffer (30 min each at room temperature). Next, sections were incubated with an anti-rabbit horseradish-peroxidase conjugated secondary antibody in TNB buffer for 10 min at room temperature.

Sections were analyzed with a Nikon Eclipse E600 Fluorescence microscope equipped with 10X objective. The GFAP labeling was quantified using the Image J Software (National Institutes of Health). In brief, the area of interest was encircled on micrographs and the sum of labeling with intensity above a set threshold was calculated by the program (raw integrated density).

3.5 ANIMALS (PAPERS I, III, IV)

Sixty male adult C57BL/6 mice (Charles River Laboratories, Inc., Sulzfeld, Germany) were used in **paper I**. In **paper III**, 36 male *Grk3*$^{-/-}$ mice (B6.129-*Adrbk2*^{tm1Rjl}/J) on a C57BL/6 background were used (The Jackson Laboratory, Bar Harbor, ME, USA, detailed in (Peppel et al., 1997)). Thirty-four *Grk3*$^{+/+}$ littermates were used as controls. In-house bred male adult C57BL6 mice were used for KYNA analysis post intracerebroventricular (ICV) IL-1β injection (n = 35), as well as in **paper IV** (n = 136). Environmental conditions were checked daily and maintained under constant temperature (25°C) and humidity (40–60 %) in a room with 12 h light/dark cycle (lights on at 06.00 hours). Food and water was provided ad libitum. Experiments were approved by and performed in accordance with the guidelines of the Ethical Committee of Northern Stockholm, Sweden. Animals tested for PPI deficits post ICV IL-1β in **paper III** were male adult C57BL6 mice. These experiments were performed and animals were housed at the University of California San Diego (UCSD).

3.6 TISSUE COLLECTION AND PREPARATION (PAPERS I – IV)

Animals were sacrificed by decapitation following isoflurane anesthesia (≈ 4 %). Blood from animals in **paper IV** was acquired by either cardiac puncture or collected from the trunk after decapitation. Blood samples were collected in eppendorf tubes and allowed to coagulate over night at 4 °C. The following day, serum was collected and centrifuged for 15 min at 1500 × g before being transferred to new eppendorf tubes and stored at -80 °C. In **paper I**, **III**, and **IV**, brains were swiftly removed from decapitated animals, and hippocampi (**paper III**) were collected. Brain tissue were immediately frozen on dry ice, collected in eppendorf tubes and stored at -80 °C.

Prior to analysis, tissue and astrocyte media (**paper II**) samples were (brain tissue: three to sevenfold (w/w), serum and astrocyte media: onefold (v/v)) diluted in 0.4 M PCA solution. Brain tissue was then homogenized by a disperser (Ultra-Turrax®, IKA, Stauffen, Germany). Brain homogenates, serum, and astrocyte media mixtures were centrifuged for 5 min at 20 000 × g and supernatants were transferred to new eppendorf tubes. Supernatants were then further 10 % diluted by the addition of pure PCA, vortexed, and centrifuged again at 20 000 × g for 5 min before being transferred to new tubes. Hippocampal tissue in **paper III** for IL-1β detection was homogenized using a Bullet Blender® (2 × 3 min, 4 °C, Next Advance inc., Averill park, NY, USA) in ice-cold lysis buffer with added protease inhibitor (no. 11836170001) and phosphatase inhibitor II and III. The homogenates were then centrifuged at 16 000 × g and 50 µl supernatant

was used for analysis. For **paper IV**, mice hemi brains were weighed and sonicated in 600 µl PBS buffer. After ultracentrifugation (30 000 × g, 4 °C), internal standards in 5 % formic acid were added to supernatants (50 µl), which were filtered (3 000 × g, 60 min) using 10kDa Ultracel®-10 filter plates (Millipore, Darmstadt, Germany). Serum samples (**paper IV**) and astrocyte media (**paper II**) were solid-phase extracted (Oasis® MAX, Waters Corporation). Before washing and elution (60% acetonitrile, 38 % methanol and 2 % formic acid) of analytes, cartridges were equilibrated and internal standards were added (in 5 % ammonium hydroxide). The organic phase was evaporated with nitrogen and redissolved in 2.5 % (serum samples), or 0.1 % (astrocyte media) formic acid.

3.7 HUMAN SUBJECTS (PAPERS II, III)

Briefly, in **paper II**, olanzapine-treated patients with schizophrenia or schizoaffective disorder were recruited during 2005 – 2007. Patients were somatically healthy at recruitment. Smoking was allowed, as well as co-medication with zopiclone and lithium. Symptoms were rated with the Brief Psychiatric Rating Scale (BPRS) and Global Assessment of Functioning (GAF) scale. Full study details have been previously published (Skogh et al., 2011) as well as methods for olanzapine analysis (Josefsson et al., 2010). Controls were collected in 2005 – 2008 among medical staff, medical students, and their relatives. These were free from somatic and psychiatric conditions as verified by a medical and psychiatric evaluation. Further, none of the healthy volunteers had a family history of serious psychiatric disorder and were medication-free for at least one month.

In **Paper III**, data from euthymic bipolar disorder outpatients were collected from the Northern Stockholm psychiatric clinic. Healthy controls were randomly selected by Statistics Sweden. Cohorts underwent the same clinical evaluation. Study details have previously been published, including diagnostics (Jakobsson et al., 2013; Olsson et al., 2012), CSF analyses (Olsson et al., 2012), and genotyping (Bergen et al., 2012). eQTL data from the HapMap2 sample was accessed through SNPexp v1.2. (http://app3.titan.uio.no/biotools/tool.php?app=snpexp). The analysis was based on an additive model. Studies were carried out according to the declaration of Helsinki. All patients and healthy volunteers received verbal and written information about the study and provided written consent.

3.8 ANIMAL SURGERY

3.8.1 Microdialysis surgery (paper III)

Mice were put in a plastic induction chamber and anesthetized with 4% isoflurane delivered by an Univentor 400 anesthesia unit (Univentor, Zejtun, Malta). When both righting reflex and response to toe pinch were absent, mice were attached to a stereotactic instrument (David Kopf Instruments, Tujunga, CA, USA). Isoflurane was continuously delivered by a nose cone and mice

body temperature were maintained at 37 °C by a heat pad (Homeothermic Blanket Control Unit 50-7053-F, Harvard Apparatus, Holliston, MA, USA). After an ocular lubricant had been applied, the head was shaved and swabbed with ethanol. A small incision (< 1 cm) was then made along the midline of the head and wound edges were retracted. The skull was then swabbed clean, and bupivacaine (5 mg/ml) was applied. A thin layer of quick-setting cyanoacrylate glue (BT AB, Stockholm Sweden) was applied to reinforce the skull and allow the cement to attach. The stereotactic instrument was then positioned according to the coordinates (hippocampus anterior/posterior (AP): -2.9 mm, medial/lateral (ML): -3.2 mm, dorsal/ventral (DV): -1.5 mm; striatum AP: +0.5 mm, ML: -2 mm, DV: -1.5 mm) and a small hole was drilled. A guide cannula (AT4.7.IC, AgnTho's AB, Stockholm, Sweden) containing a dummy probe was then inserted. The guide cannula was fixated with acrylic dental cement and allowed to settle for ≈ 5 – 10 min. Mice were given 0.5 ml saline subcutaneous (s.c.) before the wound was sutured, and animals were allowed to recover single-housed for 24 h. Stereotactic coordinates were according to the mouse brain atlas by Paxinos (Paxinos and Franklin, 2008).

3.8.2 Intracerebroventricular IL-1β injection (paper III)

3.8.2.1 Biochemical measurements

The procedure was according to microdialysis surgery up to the point of cannula insertion with the exception that no glue was applied. Here, a small glass capillary was instead positioned and inserted into the ventricle (AP: -0.34 mm, ML: -1 mm, DV: -2 mm). Four µl of IL-1β (0.125, 0.25, 1.25, or 2.5 ng/µl) was then infused over 8 min, and the capillary was allowed to stay for 5 additional min to prevent backflow of liquid. The wound was then closed with metal clips and mice were given 0.5 ml saline s.c.. Mice were sacrificed 6 h post-infusion and tissues were collected.

3.8.2.2 PPI experiments

These experiments were conducted at The University of California, San Diego (UCSD). Surgery was performed as described previously (Vinkers et al., 2007). Briefly, a stainless steel guide cannula was implanted above the lateral ventricle. Mice recovered for 5 days prior to behavioral testing. Immediately prior to PPI experiments, IL-1β or vehicle were infused through an injector in a volume of 0.5 µl. At the end of the study, cannula placement was checked via dye infusion.

3.9 PPI (PAPER III)

3.9.1 *Grk3*$^{-/-}$ mice

PPI was performed in two SR-LAB™ sound-attenuated cabinets measuring 35×33×46 cm (SD instruments, San Diego, CA, USA). An enclosed loudspeaker provided the acoustic stimuli (white noise) as background (65 dB) and tone bursts. Here, mice were placed in a plexiglass enclosure (3.7 cm in diameter) connected to a piezoelectric accelerometer (SD instruments). The accelerometer was connected to a standard personal computer running the startle analysis software (SD instruments). The same person performing the experiments handled all mice for up to a week prior to the PPI session. PPI experiments started with a baseline run consisting of four P120 trials opening and ending the session. In between there were six evenly distributed PP12P120 trials with two P120s between each. The experimental session entailed a 5 min habituation period to background noise (continuous throughout session), followed by five P120s. This was immediately followed by *a variable stimulus intensity* block **c**ontaining five trial types: P120, P110, P100, P90, and P80, each presented four times. A *variable prepulse intensity* block (**Table 2**) consisting of 12 P120 trials, and ten trials each of PP4P120, PP8P120, and PP16P120, then followed, see **Table 2**. Next, a *variable interstimulus interval* block (**Table 2**) was presented to the mice. Here, four each of the trials: ISI500, ISI200, ISI100, ISI50, and ISI25 were presented to the mice. Eight single P120s were scattered within the block. Throughout the session, NS trials were presented in between each trial. All trial types within each block were presented in a pseudo-randomized order with an average inter-trial interval of 7.5 s (not including the trials without acoustic stimulus). The session ended with five P120s for startle habituation assessment. The mean of the first 65 accelerometer readings (each 1 ms long) was defined as mean startle magnitude. Percent PPI was calculated using the formula: $\%\ PPI = ((A - B)/A) \times 100$, where A = Mean startle magnitude of P120 trials within blocks, and B = Mean startle magnitude of the prepulse+pulse trials within the same block.

Table 2.

Trial name	Intensity (dB)	Length (ms)	Interval (ms)
A. *Single pulse trials*			
P120	120	40	-
P110	110	40	-
P100	100	40	-
P90	90	40	-
P80	80	40	-
B. *Prepulse + pulse trials*			
PP16P120	16+120	20+40	80
PP12P120	12+120	20+40	80
PP8P120	8+120	20+40	80
PP4P120	4+120	20+40	80
C. *Interstimulus interval trials*			
ISI500	8+120	20+40	480
ISI200	8+120	20+40	180
ISI100	8+120	20+40	80
ISI50	8+120	20+40	30
ISI25	8+120	20+40	5
NS	-	40	-

dB are decibels over background (65dB). Interval is the time between end of prepulse and start of pulse. NS = No stimulus

3.9.2 IL-1β infused mice

These sessions were run at UCSD and have been described previously (Gresack and Risbrough, 2011). Briefly, startle testing began immediately after IL-1β infusion and continued hourly for six hours. The PPI session lasted 20 min and mice were returned to their home cage in between sessions.

3.10 LOCOMOTOR ACTIVITY (PAPER I)

Locomotor activity (LA) performance was tested in four square plexiglass containers measuring 50×50×21.6 cm (ADITECH, Fjärås, Sweden). The containers were placed inside unlit boxes that were equipped with two layers of photocells (16 per wall and level, 3.1 cm apart), creating an infrared grid allowing measurement of the factors listed in **Table 3**. Beam breaks were registered and counted by a standard personal computer. The same person performed all tests between 6 a.m. and 6 p.m. Mice were either treated with kynurenine i.p. acutely (10 mg/kg immediately prior to session (n = 20) or subchronically (100 mg/kg, twice daily for six days, n = 9). Control animals received saline i.p. (acute, n = 18; subchronically, n = 13). The experiment consisted of three 60 min LA sessions 24 h apart. The third session was considered the test session for spontaneous LA. Immediately after the third session mice received a 5 mg/kg injection of amphetamine i.p. (acute kynurenine/saline, n = 13/12; subchronic kynurenine/saline, n = 5/7) or saline i.p. (acute kynurenine/saline, n =7/6; subchronic kynurenine/saline, n = 4/5) and amphetamine-induced LA was measured for an additional 90 min. Mice were sacrificed immediately after the last session.

Table 3.

Measure	Definition
Horizontal Activity	Total count of beam breaks in the lower level
Peripheral Activity	Number of beam breaks along box walls
Forward Locomotion	New beam breaks in the lower horizontal plane
Corner Time	Accumulated time in seconds of two peripheral simultaneous beam breaks
Rearing Activity	Number of beam brakes in the upper level

3.11 MICRODIALYSIS (PAPER III)

All microdialysis experiments were performed in freely moving animals in their home cage. 24 h post-surgery, mice were tethered to a liquid swivel and the dummy probe was replaced with an AT4.7.2.PES probe (shaft length: 7 mm, membrane length: 2 mm, molecular cut-off: 6 kDa, AgnTho's AB). The probe was continuously perfused with aCSF at 1 µl/min, delivered by a Univentor 864 (Univentor Ltd). The dialysate was collected in polypropylene tubes, which was either analyzed or frozen every 30 min. Experiments started by acquiring three stable baseline readings for determination of basal extracellular KYNA or dopamine levels. Mice were then given i.p. probenecid (200 mg/kg) or amphetamine (2 mg/kg), and microdialysis sessions continued for up to six h.

3.12 LPS INJECTIONS (PAPER IV)

Animals were divided into the following groups; **i**) saline+saline **ii**) LPS+saline **iii**) LPS+LPS **iiii**) saline+LPS*. LPS was administered i.p. (0.83 mg/kg per injection). There were 16 hours between the first and second injection. Animals were sacrificed 24, 48, 72, and 120 hours after the first injection (**Figure 3**). * Group to control for time between last LPS injection and time of sacrifice in group **iii**. In addition, a group of mice received a single 1.66 mg/kg LPS to account for total dose injected in group **iii**.

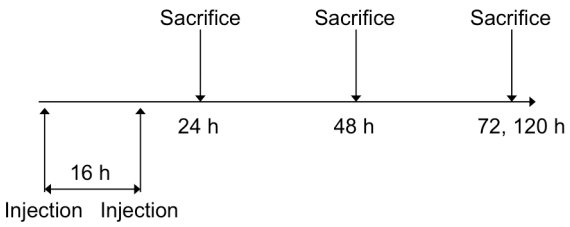

Figure 3. Treatment regime used in **paper IV**

3.13 HIGH-PERFORMANCE LIQUID CHROMATOGRAPHY (PAPERS I – V)

3.13.1 Fluorescent detection (papers I – IV)

Brain homogenates and serum samples were run through an isocratic high-performance liquid chromatography (HPLC) system. 50 µl of sample or 30 µl dialysate was manually injected into a 100 µl loop through a Rheodyne® 7725i valve (IDEX, Oak Harbor, WA, USA). The mobile phase was pumped through a 4 × 100 mm reversed-phase ReproSil 100 C18, 3 µm column (Dr. Maisch GmbH, Ammerbuch, Germany), at 0.5 ml/min. The eluate was then run through a Shimadzu SPD-10A UV-Vis detector (Shimadzu Corporation, Kyoto, Japan) set to 360 nM for quantification of kynurenine in serum samples. The mobile phase was thereafter mixed with a 0.5 M zinc acetate buffer delivered at 10 ml/h by a Pharmacia P-500 (Pharmacia, Uppsala, Sweden). Brain and serum KYNA was quantified by a Jasco FP-2020 Plus fluorescence detector (excitation wavelength: 344 nm, emission wavelength: 398 nm, bandwidth: 18 nm. Jasco Ltd., Hachioji City, Japan). Signals from the detectors were transferred to a personal computer and analyzed by Azure® (Datalys, Grenoble, France). KYNA (30 nM down to 0.156 nM) and kynurenine (5 µM to 0.156 µM) standards were run throughout the session to confirm linearity and for interpolation of unknown values. Retention times were; KYNA (7 min), and kynurenine (4 min).

3.13.2 Electrochemical detection (papers III, IV)

Twenty µl of brain homogenate samples were diluted and neutralized in 160 µl dH_20 and 20 µl 1 M NaOH. Twenty µl of neutralized homogenate or 30 µl dialysate were manually injected into an electrochemical HPLC system through a Rheodyne 7125 (IDEX) valve. The mobile phase was pumped at 0.7 ml/min by a Shimadzu LC-20AD (Shimadzu Corporation). Analytes were separated by a reversed phase Zorbax® 3.5 µm Eclipse XDB-C18, 4.6 x 150 mm column (Agilent Technologies, CA, USA). Electric currents were obtained from a Coulochem III potentiostat

(ESA Inc., Chelmsford, MA, USA) with a 500 mV applied potential that controlled a high-sensitivity ESA 5011A analytical cell (ESA Inc.). Signals were transferred to a standard personal computer running Clarity® (DataApex, Prague, The Czech Republic). Samples were quantified against a standard mixture containing 10 nM each of dopamine, HVA, DOPAC, 5-HT, and 5-HIAA. Retention times in minutes: dopamine (6), DOPAC (4), HVA (7), 5-HT (11.5), 5-HIAA (5.5).

3.14 LIQUID CHROMATOGRAPHY/MASS SPECTROMETRY (PAPERS II, IV)

Brain sample filtrates (**paper IV**) were injected (7.5 µl) into an ACQUITY HPLC system (Waters Corporation, Milford, MA, USA) equipped with a SymmetryShield™ RP18 2.1 × 100 mm, 3.5 µm particle column (Waters Corporation). The mobile phase was run at 300 µl/min and was 2.1% formic acid in MilliQ water (A phase) and 95% acetonitrile, 0.1% formic acid (B phase) starting with 5% B in A for 2 min and followed by gradient elution, total run time of 10 min. Retention times for QUIN, kynurenine, and tryptophan were 1.1, 1.6, and 3.5 minutes respectively. Extracted serum samples (**paper IV**) and astrocyte media (**paper II**) were injected in the same manner (7.5 µl) into an ACQUITY HPLC. Here, the system was equipped with an HSST3 2.1 × 100 mm, 1.8 µm particle column (Waters Corporation). The mobile phases used here were of the same composition as previously and were run at the same flow rate. The run was started with 2 % B phase in A for 2 min followed by gradient elution and total run time was 15 min. Retention times were: QUIN (1.5 min), kynurenine (3.9 min), tryptophan (5.9 min), and 5-HT (3.6 min).

Detection was performed using a Xevo TQ-S triple quadrupole mass spectrometer (Waters Corporation) operating in positive ionization MS/MS configuration. The mass spectrometer was tuned for all analytes and the mass spectral transitions were set at m/z 168> 106; 209>146; 205 > 118, 190>116 and 177 > 115 and for the internal standard 172> 110 ($^{13}C_3{}^{15}N_1$-QUIN), 213>150 (D_4-kynurenine), 210 > 123 (D_5-tryptophan), and 181>118 (D_4-5-HT). Standards of each analyte were used to establish a linear calibration curve and plotted using the ratio of analyte peak area over internal standard peak area after integration by Masslynx 4.1 software (Waters Corporation).

3.15 ELECTROCHEMILUMINESCENT DETECTION (PAPERS II, III)

Analyses were performed as per manufacturers protocol on a Sector Imager 2400 (Meso Scale Diagnostics, Rockville, MA, USA). A customized Human Ultra-Sensitive 10-Plex Kit was employed in **paper II** and a Mouse ProInflammatory 7-Plex Tissue Culture Kit in **paper III** (both from Meso Scale Diagnostics). Lowest levels of detection were: 0.06 pg/ml (**paper II**), 0.04 pg/ml (**paper III**) for IL-1β, and 0.26 pg/ml (IL-6, **paper II**). Samples were run in duplicates.

3.16 STATISTICS

Analyses were performed using Prism® 6 (GraphPad Software) for Mac OS X, unless otherwise stated. Tests were two-tailed and p values < 0.05 were considered significant unless specifically stated otherwise.

3.16.1 Paper I

Spontaneous LA data were analyzed with the Mann-Whitney test or an unpaired t-test. Comparisons were done on area under the curve (AUC) data from time points between 35 – 60 min post kynurenine or saline injections. Amphetamine-induced LA data were analyzed with two-way analysis of variance (ANOVA, pretreatment × challenge), on AUC between 0 – 90 min post amphetamine or saline challenge. Whole-brain KYNA comparisons were done with the Mann-Whitney test. Comparisons were done with Prism® 4 and presented as mean ± SEM.

3.16.2 Paper II

Comparisons of cytokines and kynurenines between patients and controls were performed using the Mann-Whitney test. Levels are expressed as median and interquartile range. Age-adjusted calculations were performed with SPSS statistics (IBM Corporation, Armonk, NY, USA) using logistic regressions with age as a covariate and groups as dependent variable. For associations between patient variables, Spearman's rank correlation analyses were performed with SPSS statistics (IBM corporation). Levels of KYNA in astrocyte media were compared to controls within each time point using one-way ANOVAs with Bonferroni corrections. Data are here mean ± SEM.

3.16.3 Paper III

Differences in % PPI were evaluated with repeated measures two-way ANOVAs using prepulse intensity or interstimulus interval as the repeated measure, and genotype or treatment as between group factors. To account for multiple testing Tukey's post-hoc test was used. In the microdialysis experiments, the mean of the three first samples was considered baseline, all other sample levels were expressed as the percentage of deviation from this mean. Within groups (pre vs. post-drug) comparisons were done using repeated measures one-way ANOVA. Between group comparisons ($Grk3^{+}/^{+}$ vs. $Grk3^{-}/^{-}$) was done with repeated measures two-way ANOVA (genotype × time). Post-hoc Bonferroni corrections were used in both cases. The Mann-Whitney nonparametric test was used to compare P2X7 levels in membrane fractions, hippocampal IL-1β levels, levels of basal kynurenines, and the average startle magnitude in PPI experiments. The parametric t-test was used for comparisons between groups in the immunohistochemistry experiments.

3.16.4 Paper IV

Comparisons of brain and serum kynurenines, 5-HT, dopamine, and their metabolites were performed using the Kruskal-Wallis non-parametric test. Dunn's Post-hoc test was used to correct for multiple comparisons. Values are here mean ± SEM.

4 RESULTS AND DISCUSSION

4.1 PAPER I

Patients with schizophrenia display increased central levels of KYNA as well as amphetamine-induced dopamine release as evidenced by increased [^{11}C] raclopride receptor displacement (see 1.5; The dopamine and glutamate hypothesis). In this paper, we aimed to further explore this relationship by studying the effect of elevated KYNA on spontaneous and amphetamine-induced locomotion in mice.

4.1.1 Acute kynurenine administration

Mice treated acutely with i.p. kynurenine (10 mg/kg, n = 20) 60 min prior to open-field trials displayed increased anxiety in comparison to vehicle (n = 19) treated mice. This was shown by increased amount of time spent in corners (Mann-Whitney, p = 0.02, **Figure 4A**, and increased percentage of peripheral activity (t-test, p = 0.03, **Figure 4B**). Other parameters tested tended to decrease by acute kynurenine treatment but did not reach statistical significance (horizontal activity, p = 0.10, forward locomotion, p = 0.08, rearing activity, p = 0.09). Acute kynurenine did not augment amphetamine-induced LA (data not shown).

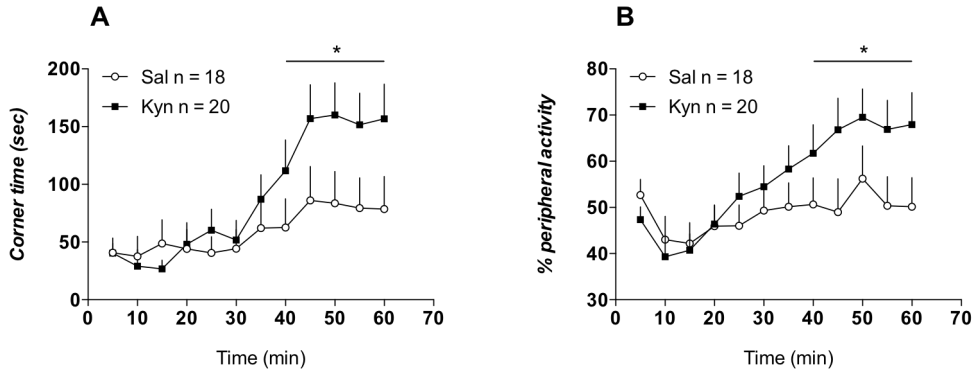

Figure 4. Corner time (**A**) and % peripheral activity (**B**) in mice treated acutely with kynurenine (Kyn, 10 mg/kg, i.p.) versus controls given saline (Sal). Area under the curve 35 – 60 min post-injection was used for statistics. * = $p < 0.05$, (**A**) Mann-Whitney, (**B**) t-test.

4.1.2 Subchronic kynurenine administration

In contrast to acute treatment with kynurenine, mice treated subchronically with kynurenine (100 mg/kg twice daily, i.p.) did not display increased anxiety in open-field trials. Further, subchronic treatment with kynurenine potentiated an amphetamine (5 mg/kg) challenge. Here, interactions (pretreatment × challenge) were significant for the measures: horizontal activity (p = 0.01, **Figure 5A**), forward locomotion (p = 0.005, **Figure 5B**), and rearing activity (p = 0.01, **Figure 5C**).

Post hoc tests were significant between pretreatment (kynurenine versus saline) groups in all three measures (Bonferroni, $p < 0.01$). These data are in line with previous experiments, where rats treated with kynurenine subchronically, but not acute, displayed augmented amphetamine-evoked dopamine release (Olsson et al., 2009).

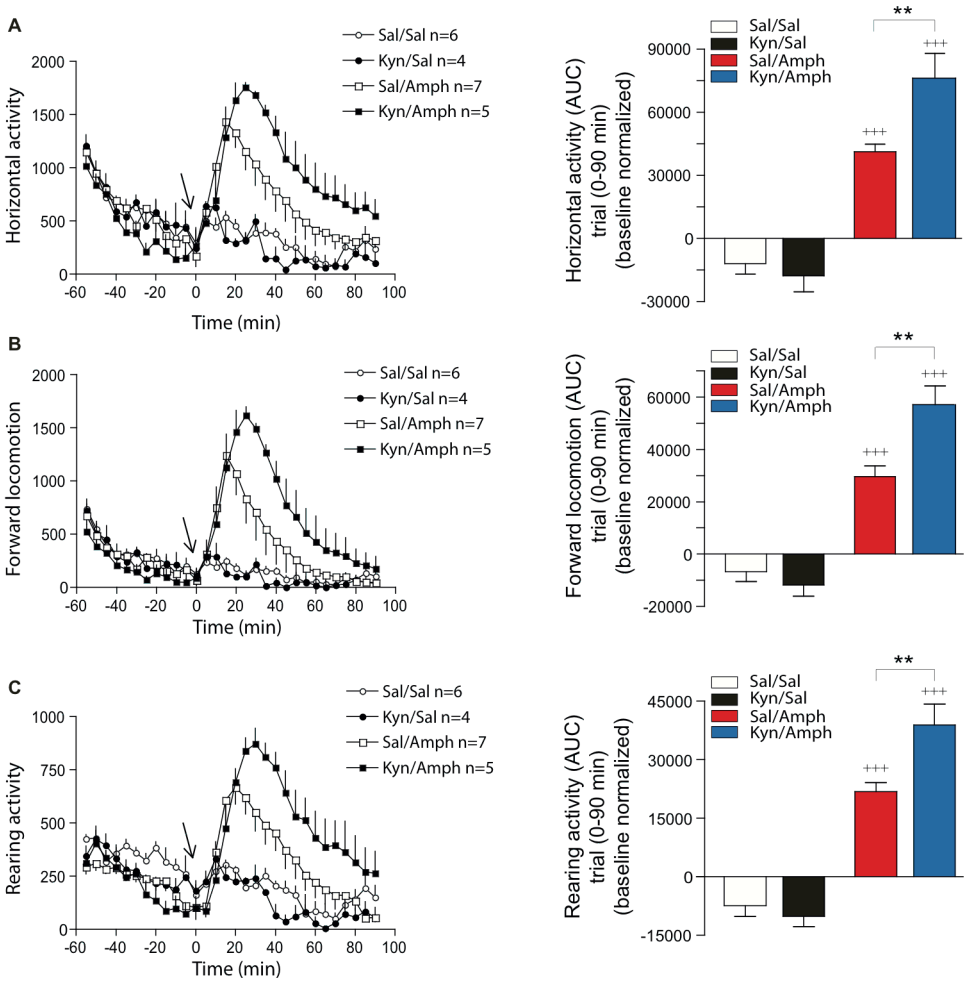

Figure 5. Differences in (**A**) horizontal activity, (**B**) forward locomotion, and **(C)** rearing activity in mice subchronically treated with kynurenine (Kyn, 2 × 100 mg/day). Amphetamine was injected at time = 0. Saline (Sal) was used as control. Bars represent area under the curve between time 0 – 90 min (mean ± SEM). ** = $p < 0.01$, $^{+++}$ = $p < 0.001$ (versus respective saline challenge). Two-way ANOVA (pretreatment × challenge) with Bonferroni corrections.

4.2 PAPER II

In this paper, a well-characterized cohort of patients was analyzed with respect to CSF cytokines and compared to healthy controls. Associations between IL-6 and previously measured kynurenines were also explored, as well as the effects of IL-6 application on the synthesis of kynurenine and KYNA in cultured human fetal astrocytes.

4.2.1 CSF levels of IL-6 and IL-8 in patients

CSF IL-6 was reliably detected in 21 patients with schizophrenia and in all healthy controls (n = 37). IL-8 was detected in 22 patients and in 36 controls. Comparisons between groups revealed significantly higher IL-6 levels in patients (2.68 pg/ml, IQR 1.80 – 3.99, versus 1.5 pg/ml IQR 1.01 – 2.25, $p < 0.001$, **Figure 6A).** After stratifying by gender, IL-6 levels were still higher in both male (2.68 pg/ml, IQR 1.67 – 3.88, n = 15), and female patients (3.25 pg/ml, IQR 1.92 – 5.83, n = 6) compared to respective controls (males: 1.12 pg/ml, IQR 0.85 – 1.68, n = 23, p = 0.006, females: 1.76 pg/ml IQR 1.41 – 2.59, n = 14, p = 0.026). IL-8 levels did not differ between groups (**Figure 6B**). Correlation analyses were then performed to rule out the possibility of age confounding. Here, neither IL-6 nor IL-8 correlated with age and comparisons between groups were still significant after adjusting for age.

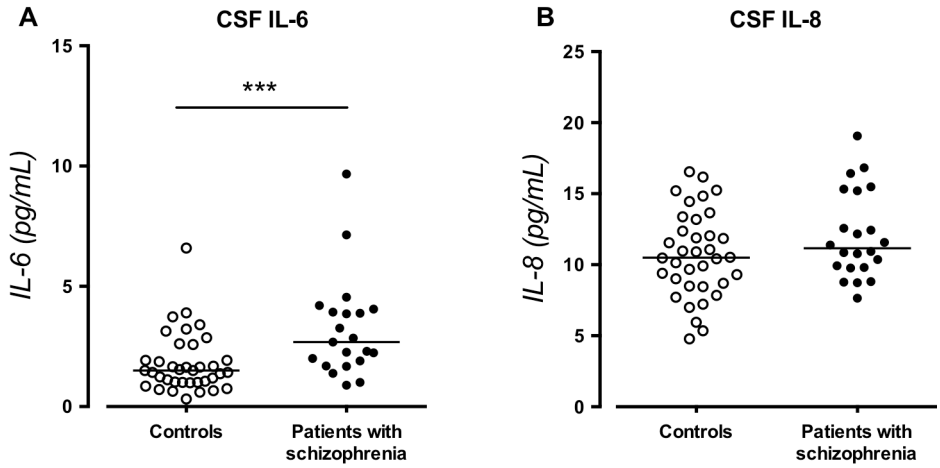

Figure 6. Cerebrospinal fluid (CSF) levels of interleukin (IL)-6 (**A**) and IL-8 (**B**) in patients with schizophrenia (IL-6, n = 21; IL-8, n = 22) compared to healthy controls (IL-6, n = 37; IL-8, n = 36). Horizontal bars are medians. *** = $p < 0.001$ (Mann-Whitney).

4.2.2 Analyses of tryptophan metabolites

In accordance with previous studies (see introduction for overview), CSF levels of KYNA (1.87 nM, IQR 1.63 – 2.29) and kynurenine (57.88 nM, IQR 48.0 – 71.3) were higher in patients (n = 23) as revealed by age-adjusted comparisons to controls (n = 37, KYNA: 1.50 nM, IQR 1.14 – 1.92, p = 0.006; kynurenine: 32.22 nM, IQR 26.2 – 49.0, p = 0.04). Tryptophan levels did not differ between groups, however, there was an increased activity in the kynurenine pathway in patients, indicated by significantly decreased tryptophan:kynurenine, and tryptophan:KYNA ratios (age-adjusted, data not shown). Further correlational analyses also showed a significant association between IL-6 levels and the tryptophan:KYNA ratio in patients only (r = -0.49, p = 0.024).

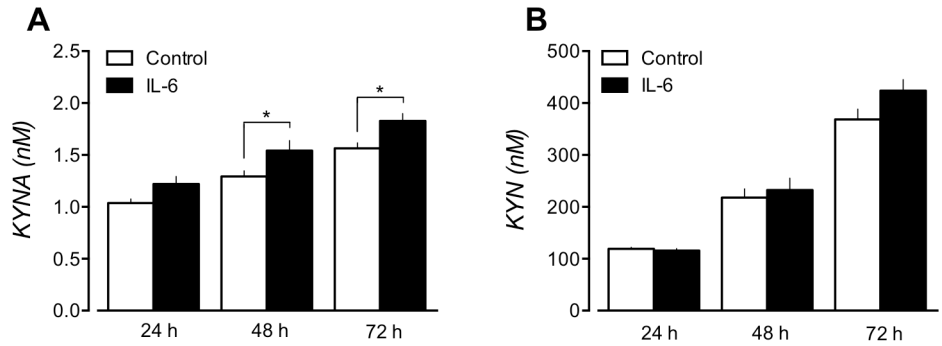

Figure 7. Kynurenic acid (KYNA) (**A**) and kynurenine (KYN) (**B**) levels (mean ± SEM) in cell media from cultured astrocytes treated with interleukin (IL)-6 or vehicle. Media was collected after 24, 48, and 72 h post-treatment. * = $p < 0.05$, one-way ANOVA with Bonferroni corrections versus vehicle within each time point.

4.2.3 IL-6 induced production of KYNA in astrocytes

To further investigate the putative connection between IL-6 and activation of the kynurenine pathway, astrocytes were treated with IL-6 and cell media concentrations of KYNA and kynurenine were analyzed for up to 72 h post-administration. Analyses showed increased production of KYNA in astrocytes at 48 h (n = 6, IL-6: 1.55 ± 0.097 nM; Control: 1.29 ± 0.054 nM) and at 72 h (n = 5, IL-6 1.83 ± 0.070 nM; Control: 1.56 ± 0.053 nM) after treatment with IL-6 compared to vehicle treated cells ($p < 0.05$, **Figure 7A**). There was no effect on the levels of kynurenine at any time point (**Figure 7B**).

4.3 PAPER III

In paper III, the functional effects of GRK3 gene deletion were studied in mice using relevant behavioral paradigms for schizophrenia. Further, effects of allelic variants of GRK3 on CSF KYNA in healthy controls and on the history of psychosis in bipolar disorder patients were explored.

4.3.1 Identification of SNPs associated with schizophrenia

The Psychiatric Genetic Consortium (PGC) database was searched for single nucleotide polymorphisms (SNPs) in proximity to the GRK3 gene. Here, the SNP with the strongest association to the schizophrenia phenotype (rs478655, OR = 0.91, MAF = 0.29, $p = 4.8 \times 10^{-4}$), located within the promoter region of GRK3, was further analyzed with regard to expression. In the HapMap2 database, the minor T allele of rs478655 was associated with increased GRK3 expression (additive model; $\beta = 0.051$, $p = 0.026$, mean T/T (n = 31) = 7.712, T/C (n = 104) = 7.584, C/C (n = 112) = 7.575).

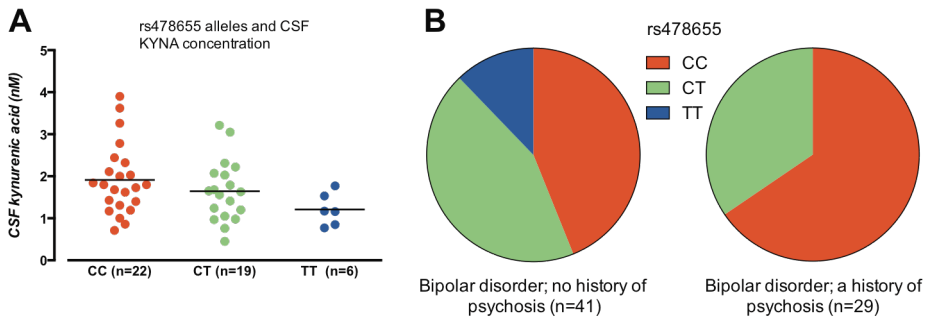

Figure 8. (**A**) Cerebrospinal fluid (CSF) levels of kynurenic acid between rs47655 haplotypes ($\beta = -0.33$, $p = 0.041$). (**B**) T/T haplotype frequency in bipolar patients stratified by history of psychosis (OR = 0.39, MAF = 0.33, $p = 0.03$).

In order to investigate the functional allele effect with regard to psychotic disorders, the rs478655 allele effect on KYNA levels was tested in a genotyped cohort of healthy individuals. This was performed as KYNA previously have been shown to be associated with psychosis (see 1.3; Kynurenic acid and schizophrenia). Here, the T/T haplotype, which was associated with increased GRK3 expression in the HapMap2 database, was associated with decreased levels of CSF KYNA ($\beta = -0.33$, $p = 0.041$, **Figure 8A**). Additional support for allele association with psychosis was revealed when the bipolar patients were stratified by history of psychosis. The minor T allele was here shown to be associated with decreased risk for psychosis (OR = 0.39, MAF = 0.33, $p = 0.03$, **Figure 8B**).

4.3.2 P2X7 membrane levels in *Grk3*$^{-}$*/*$^{-}$ mice

The assumed disrupted P2X7 internalization process by GRK3 loss-of-function was studied in *Grk3*$^{-}$*/*$^{-}$ mice. Here, P2X7 internalization was investigated by separating whole-brain derived cell homogenate into subcellular and plasma membrane fractions. P2X7 levels were thereafter determined by western blot and normalized to β-actin. *Grk3*$^{-}$*/*$^{-}$ animals displayed significantly decreased P2X7 levels in internal membrane fractions compared to *Grk3*$^{+}$*/*$^{+}$ littermates (*Grk3*$^{-}$*/*$^{-}$: 0.87 ± 0.091, n = 5; *Grk3*$^{+}$*/*$^{+}$: 1.73 ± 0.43, n = 6, p = 0.017, **Figure 9B**). Plasma membrane levels of P2X7 were higher in *Grk3*$^{-}$*/*$^{-}$ mice but did not reach statistical significance (**Figure 9A**).

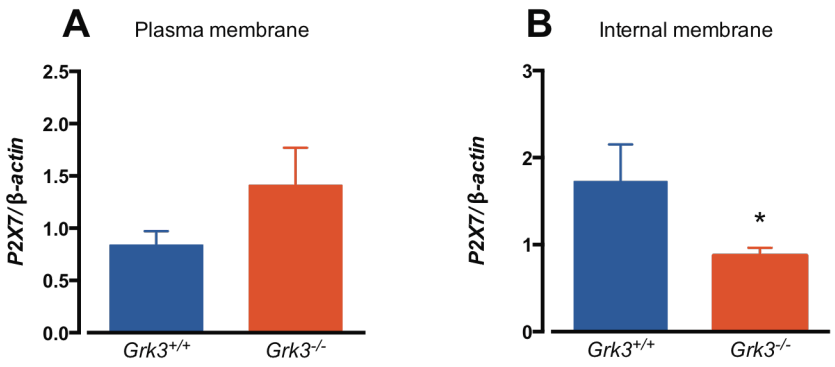

Figure 9. P2X7 levels in plasma membrane fractions (**A**) and internal membrane fractions (**B**) from *Grk3*$^{-}$*/*$^{-}$ (n = 6) mice whole-brain compared to *Grk3*$^{+}$*/*$^{+}$ littermates (n = 5). Data are mean ± SEM. * = p < 0.05 (Mann-Whitney)

4.3.3 Hippocampal IL-1β levels in *Grk3*$^{-}$*/*$^{-}$ mice

P2X7-induced caspase activation is a key mediator to subsequent IL-1β release (see 1.2.2; The P2X7 receptor. Experiments were thereafter carried out to investigate whether the disrupted P2X7 internalization seen in *Grk3*$^{-}$*/*$^{-}$ gave rise to increased IL-1β levels. Drug-naïve *Grk3*$^{-}$*/*$^{-}$ mice were euthanized and IL-1β levels in hippocampal tissue was measured by chemoluminescence (Meso scale). The levels of IL-1β were found to be significantly higher in *Grk3*$^{-}$*/*$^{-}$ mice (0.76 ± 0.093 pg/ml, n = 5) compared to *Grk3*$^{+}$*/*$^{+}$ animals (0.37 ± 0.066 pg/ml, n = 5, p = 0.008, **Figure 10**).

4.3.4 ICV IL-1β administration in C57BL6 mice

In agreement with previous unpublished data showing that IL-1β induces TDO and increases astrocyte KYNA production (Sellgren et al., 2015), brains from C57BL6 mice contained significantly higher levels of KYNA after ICV IL-1β. Mice were sacrificed six hours post-injection (IL-1β: 9.46 ± 1.88 nM, n = 7, versus vehicle: 3.50 ± 0.49 nM, n = 8, p < 0.001, **Figure 11**).

The increase seen here at the 0.5 ng dose, but not at higher doses may be explained by KMO and / or kynureninase activation (see 1.3.1; The kynurenine pathway, and Zunszain et al., 2012) at doses above 0.5 ng. In addition, the effects of IL-1β on hippocampal dependent memory appears follow an inverted U-shape pattern (Goshen et al., 2007).

Figure 10

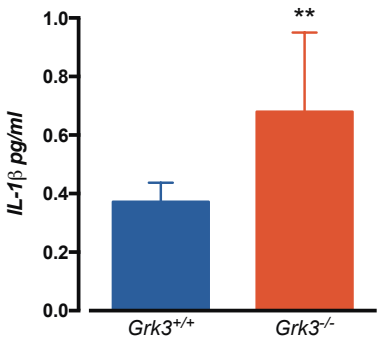

Figure 11

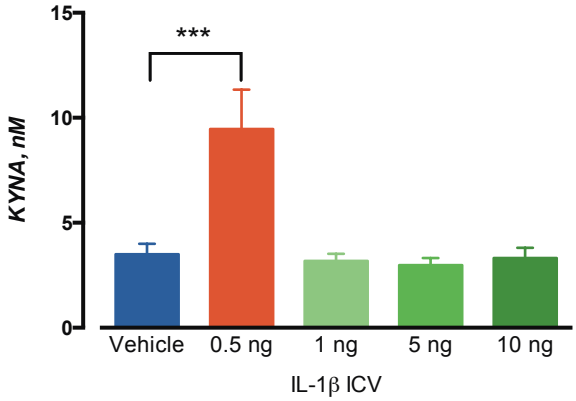

Figure 10. Hippocampal Interleukin (IL)-1β levels in *Grk3*$^{-/-}$ (n = 5) mice compared to *Grk3*$^{+/+}$ littermates (n = 5). Bars are mean ± SEM. ** = $p < 0.01$ (Mann-Whitney). **Figure 11.** Kynurenic acid (KYNA) levels in whole-brain from C57BL6 mice administered IL-1β intracerebroventricular (ICV) in escalating doses (n = 6 – 8). *** = $p < 0.001$ (One-way ANOVA with Bonferroni corrections).

4.3.5 PPI

4.3.5.1 Grk3$^{-/-}$ *mice*

In the variable prepulse intensity block, *Grk3*$^{-/-}$ mice displayed decreased PPI as evident by a significant genotype × prepulse intensity interaction ($F(2, 74) = 4.20$, $p < 0.05$). Post-hoc comparisons further revealed significantly lower % PPI in *Grk3*$^{-/-}$ mice at the 73 dB prepulse level (eight dB over background) compared to *Grk3*$^{+/+}$ littermates (*Grk3*$^{-/-}$: 36.87 ± 5.17, n = 19, versus *Grk3*$^{+/+}$: 50.44 ± 3.56, n = 20, $p < 0.05$, **Figure 12B**). There was no difference between genotypes in basal startle magnitude (**Figure 12A**), nor in the variable interstimulus interval block (data not shown).

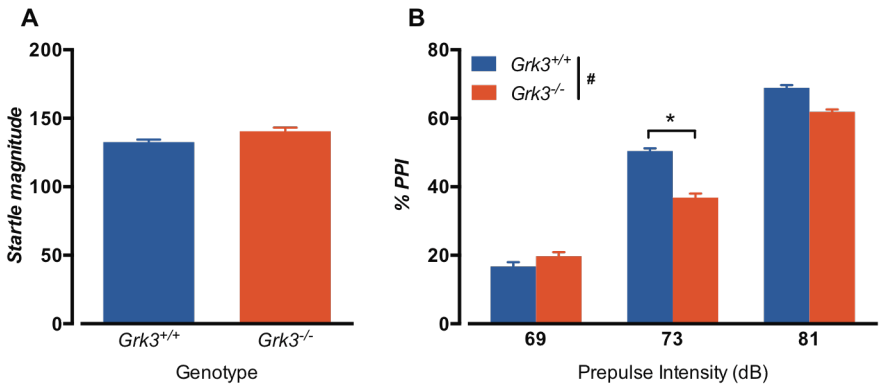

Figure 12. Average (± SEM) startle magnitude (**A**) and percent prepulse inhibition (PPI, **B**) in *Grk3*$^{-/-}$ mice (n = 19) compared to *Grk3*$^{+/+}$ littermates (n = 20). (**A**) Startle magnitude was 120 dB and (**B**) prepulses 69, 73, and 81 dB, after which a single 120 dB pulse followed. $^{\#}$ = $p < 0.05$, two-way repeated measures ANOVA (genotype × prepulse level). * = $p < 0.05$, Tukey´s post-hoc test.

4.3.5.2 ICV IL-1β administration

In similarity to the *Grk3*$^{-/-}$ mice, a low dose of ICV administered IL-1β decreased PPI across hours 1 – 3 post-infusion in C57BL6 mice (0.5 ng: 22.06 ± 4.24 nM versus vehicle: 38.31 ± 5.57, $p < 0.05$, Bonferroni's post-hoc, **Figure 13A**). Throughout the six h session there was a significant decrease in % PPI in mice administered 0.5 ng IL-1β (main effect of drug, $p = 0.0345$, **Figure 13B**).

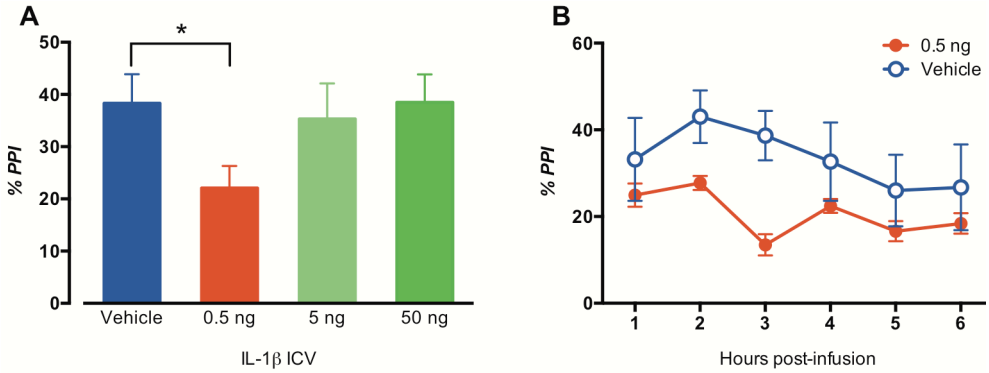

Figure 13. (**A**) Average (± SEM) percent prepulse inhibition (PPI) in C57BL6 mice receiving interleukin (IL)-1β intracerebroventricular (ICV). Data are collapsed across hour 1 – 3 post infusion. (**B**) Average (± SEM) percent PPI in mice receiving 0.5 ng IL-1β tested hourly over 6 h. * = $p < 0.05$, two-way repeated measures ANOVA (treatment × prepulse level) with Tukey corrections.

4.3.6 Microdialysis

4.3.6.1 Probenecid administration in Grk3$^{-/-}$ mice

As IL-1β induces the kynurenine pathway in vitro (see 1.3.2; Regulation of the kynurenine pathway) and in vivo (see 4.3.4; ICV IL-1β administration in C57BL6 mice), *Grk3*$^{-/-}$ mice brains were analyzed with regard to kynurenine and KYNA content. Here, *Grk3*$^{-/-}$ mice display higher basal hippocampal levels of kynurenine versus *Grk3*$^{+/+}$ mice (115.2 ± 5.74 nM, n = 7, versus 96.19 ± 3.3 nM, n = 8, p = 0.0140). Further, no difference in basal KYNA level between genotypes was found (data not shown). However, when inhibiting brain KYNA efflux by probenecid (200 mg/kg, i.p.), there was a significantly higher KYNA accumulation in *Grk3*$^{-/-}$ mice compared to *Grk3*$^{+/+}$ littermates as measured by microdialysis (**Figure 14A**).

4.3.6.2 Amphetamine administration in Grk3$^{-/-}$ mice

Patients with schizophrenia display increased dopamine release in response to amphetamine compared to healthy controls (see 1.5; The dopamine and glutamate hypothesis). Difference in amphetamine responsiveness between *Grk3*$^{-/-}$ and *Grk3*$^{+/+}$ mice was here investigated my means of microdialysis. In this setting, *Grk3*$^{-/-}$ mice displayed increased striatal dopamine compared to *Grk3*$^{+/+}$ littermates (**Figure 14B)**.

4.3.7 Immunohistochemistry

Staining for the astrocytic marker GFAP revealed significantly higher immunoreactivity in *Grk3*$^{-/-}$ mice compared to *Grk3*$^{+/+}$ animals in the hippocampus (≈ bregma -1.46, p = 0.037, **Figure 15** top panel), cerebral peduncle (p = 0.037, **Figure 15** middle panel), thalamus (p = 0.005, **Figure 15** bottom panel), and paraventricular hypothalamus (p = 0.044, not shown). Staining for the microglial markers ionized calcium binding adaptor molecule (Iba)-1 or cluster of differentiation molecule (CD)11b showed no difference between genotypes (data not shown), collectively indicating a specific elevated astrocytic immunoreactivity in *Grk3*$^{-/-}$ mice.

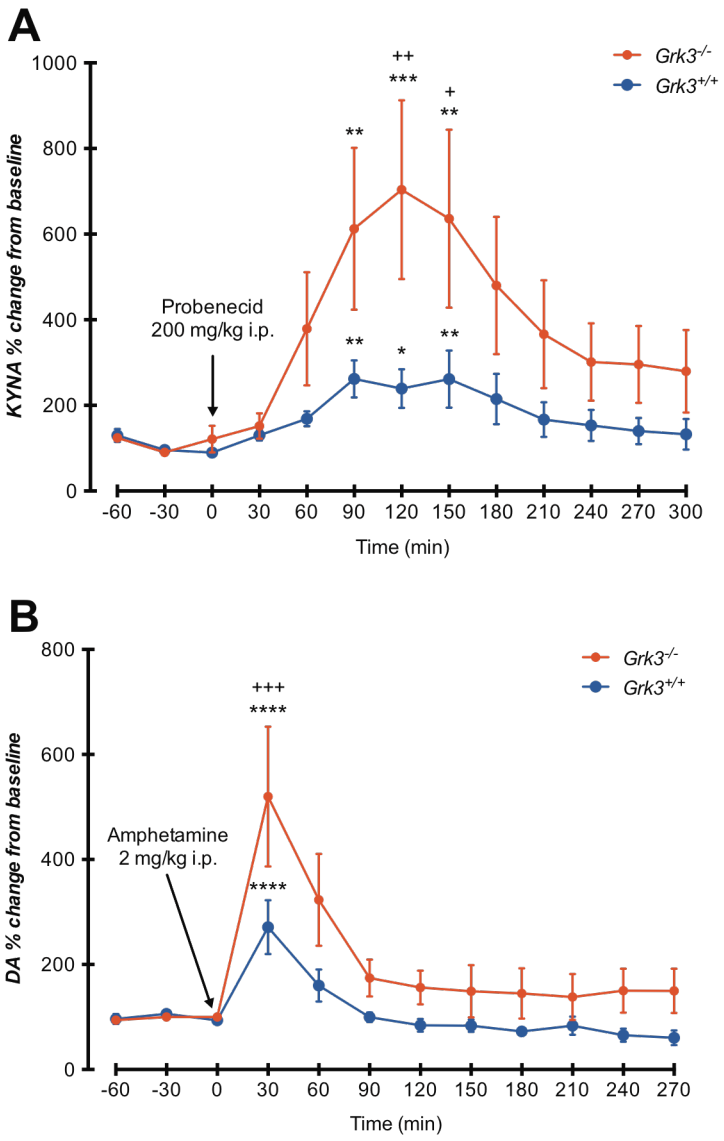

Figure 14. Change in hippocampal kynurenic acid (KYNA, **A**) and striatal dopamine (DA, **B**) after i.p. administration of (**A**) probenecid or (**B**) amphetamine to *Grk3*$^{-/-}$ mice (**A**, **B**, n = 5) versus *Grk3*$^{+/+}$ littermates (**A**, n = 6, **B**, n = 5). Datapoints are mean ± SEM percent change versus pre-drug value. **** = $p < 0.0001$, *** = $p < 0.001$, ** = $p < 0.01$, * = $p < 0.05$, one-way repeated measures ANOVA with following Bonferroni corrections compared to pre-drug value. +++ = $p < 0.001$, ++ = $p < 0.01$, + = $p < 0.05$, two-way repeated measures ANOVA (genotype × time) with Bonferroni corrected comparisons between genotypes.

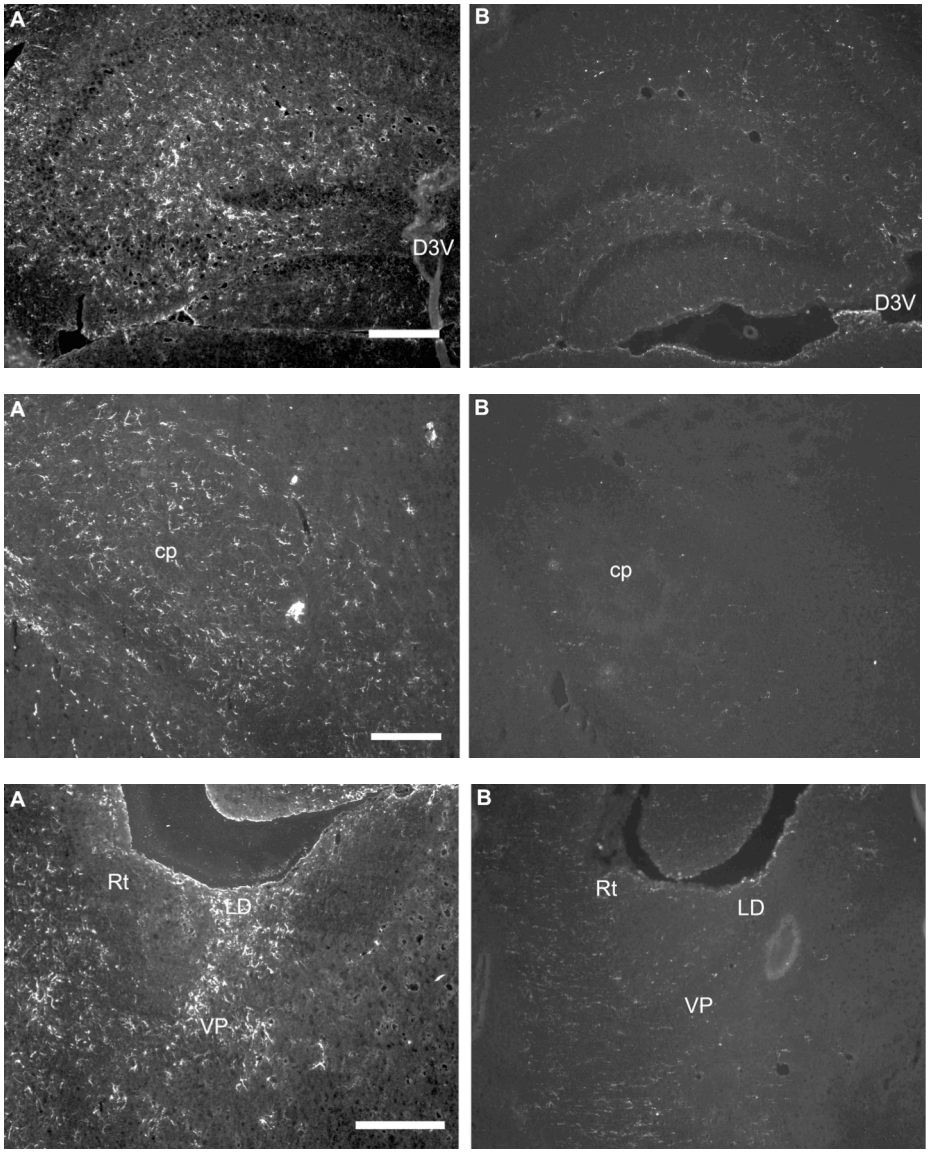

Figure 15. GFAP stained hippocampus (D3V = dorsal third ventricle, top panel), cerebral peduncle (cp, middle panel), and thalamus (Rt = Reticular, LD = laterodorsal, VP = ventral posterior, bottom panel). (**A**, *Grk3*$^{-/-}$ **B**, *Grk3*$^{+/+}$). Scalebar = 200 μm

4.4 PAPER IV

The effects of single and dual injections of LPS (0.83 mg/kg per injection) were investigated with regard to central and peripheral levels of kynurenines, dopamine, and 5-HT with their respective metabolites. Results showed that dual, but not single LPS injections affected brain and serum levels of KYNA, brain QUIN (**Figure 16 C, D, E, F**), and serum tryptophan (**Figure 16 H**). The effect on KYNA seem to be regimen-dependent as no dose-response pattern was seen and mice receiving a single 1.66 mg/kg LPS injection did not display elevated brain KYNA (data not shown). Brain and serum kynurenine and brain tryptophan were affected by both LPS regimens (**Figure 16 A, G, B**).

Indications of increased brain IDO and/or TDO activity was present at all time points after dual LPS as reflected by an increased kynurenine:tryptophan ratio. A single LPS injection increased the kynurenine:tryptophan ratio at time points, 24 and 120 hours (data not shown).

Brain dopamine and 5-HT was unaffected by both treatment regimens (data not shown. However, turnover was affected as evident by increased HVA:dopamine, and 5-HIAA:5-HT ratio at the 24 and 48 hour timepoint by dual LPS injections, and at 24 hours by single LPS.

Data show that the response to LPS with respect to kynurenines is altered depending on injection regimen. Here, only dual LPS elevated brain KYNA and QUIN. The effects seen here may have numerous causes such as facilitated passage of peripheral cytokines or kynurenine across the BBB induced by LPS. LPS induces BBB permeability (Jangula and Murphy, 2013) while only entering the brain in trace amounts (Banks and Robinson, 2010). In addition, LPS induces cytokine release from endothelial cells lining the BBB (Reyes et al., 1999) and facilitates BBB adhesion and transport of immune cells (de Vries et al., 1994; Persidsky et al., 1997).

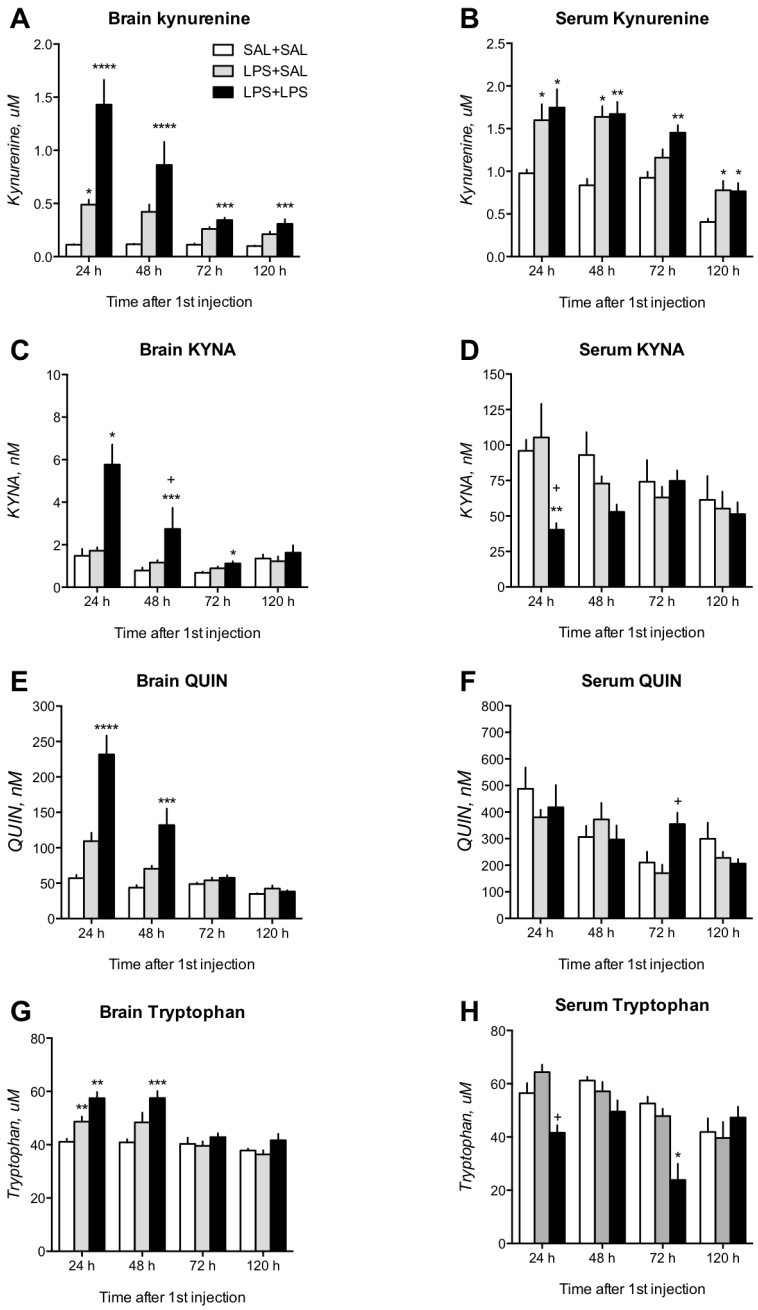

Figure 16. Levels (mean ± SEM) of kynurenine (**A**, **B**), kynurenic acid (KYNA **C**, **D**), quinolinic acid (QUIN **E**, **F**), and tryptophan (**G**, **H**) in the brain (**A**, **C**, **E**, **G**) and serum (**B**, **D**, **F**, **H**) in mice receiving single (grey bars) and dual (black bars) LPS (0.83 mg/kg/injection) injections. **** = $p < 0.0001$, *** = $p < 0.001$, ** = $p < 0.01$, * = $p < 0.05$, versus controls (white bars). + = $p < 0.05$, versus single LPS. Kruskal Wallis with Dunn corrections. n = 6 – 8 in each group.

5 GENERAL DISCUSSION

Data presented in this thesis suggest that GRK3 is as a putative contributor to psychosis. Thus, GRK3 expression was found to associate with CSF KYNA levels and with psychosis in patients with bipolar disorder. GRK3 participates in inflammatory signaling by inhibiting P2X7 dependent IL-1β activation (**Figure 17**). Loss of function in GRK3 would consequently lead to increased immune signaling. Testing for such consequences was therefore carried out in *Grk3*$^{-/-}$ mice.

In *Grk3*$^{-/-}$ mice, signs of decreased P2X7 internalization were seen. This decrease would hypothetically lead to excess caspase-1 stimulation, causing increased IL-1β release. Indeed, measurements of hippocampal IL-1β in *Grk3*$^{-/-}$ mice were in line with this.

Building from previous data showing that IL-1β induce KYNA levels in astrocytes (Sellgren et al., 2015), C57BL6 mice here ICV injected with IL-1β displayed increased levels of brain KYNA. In addition, it was demonstrated that the induction of brain KYNA by LPS is treatment regimen dependent. While a single injection of LPS did not influence brain KYNA, mice receiving dual injections displayed marked elevations. The reasons for these disparate changes in KYNA are yet unknown but may include increased permeability of the BBB to peripheral kynurenines and cytokines.

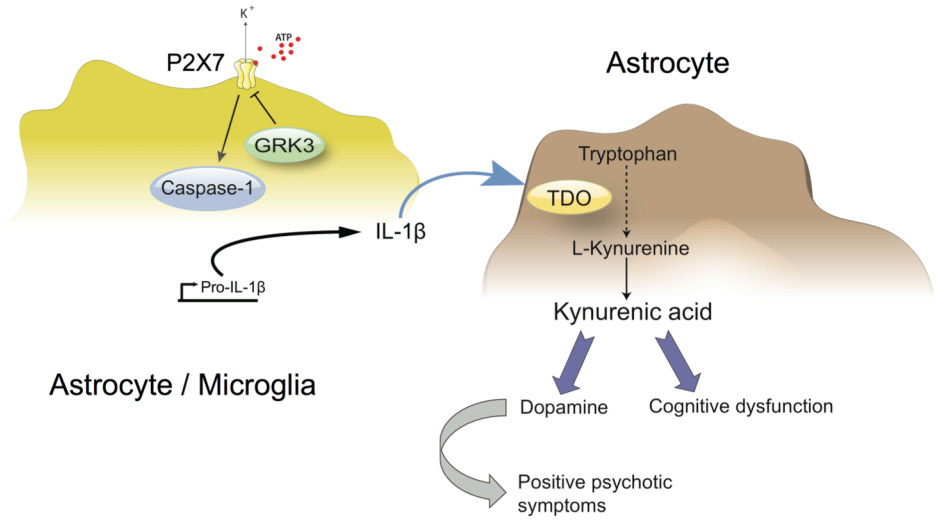

Figure 17. GRK3 Loss of function leading to increased activation of the kynurenine pathway via IL-1β. Activation of the kynurenine pathway is suggested to induce symptoms associated with psychotic disorders, including schizophrenia.

Testing for a schizophrenia-like phenotype in *Grk3*$^{-/-}$ mice revealed deficits in PPI, possibly related to the increased turnover of KYNA, as elevated levels of KYNA have previously been shown to induce such deficits (Erhardt et al., 2004), and that ICV administration of IL-1β increase KYNA and cause similar reduction in PPI. Furthermore, *Grk3*$^{-/-}$ mice display elevated hippocampal kynurenine levels in addition to the increased KYNA turnover.

The connection previously shown between KYNA and dopamine was further strengthened as *Grk3*$^{-/-}$, and mice with subchronically elevated brain KYNA levels showed an augmented response to amphetamine. This was verified by increased striatal dopamine release (*Grk3*$^{-/-}$) and increased locomotor activity in mice with elevated KYNA. These results provide a functional link between the abundant evidence on dopaminergic dysfunction and elevated KYNA in schizophrenia.

In addition, patients with schizophrenia displayed increased CSF levels of IL-6, further strengthening the hypothesis of immune activation in schizophrenia. In addition, an intimate relationship between IL-6 and the schizophrenia-linked kynurenine pathway is suggested based on the correlations found in patients, and the KYNA inducing properties of IL-6 in astrocytes. Interestingly, only IL-6 was found to be elevated in these chronic patients, in contrast to the selective increase of IL-1β previously shown in first-episode patients (Söderlund et al., 2009).

Collectively, thesis data demonstrate that mice with subchronically elevated levels of KYNA, or lacking GRK3 display multiple functional deficits further underlining the involvement of KYNA and inflammatory signaling in the pathophysiology of schizophrenia.

6 ACKNOWLEDGEMENTS

First and foremost, a big thank you to my main supervisor, Associate Professor **Sophie Erhardt,** your never ceasing enthusiasm and knowledge really made this thesis possible. Thank you also for always having your office door open even though it encouraged the asking of stupid questions while passing by.

A big thank you also to my kind and patient co-supervisor, Dr. **Lilly Schwieler**, whom with great devotion showed me all the do´s and don'ts in animal handling. Thank you also for encouraging talks and your positive spirit.

And last, but certainly not least, thank you Professor **Göran Engberg,** for accepting me as a masters project student years ago. And for your vivid and inspiring introduction talk to the fascinating world of kynurenines.

Thank you, **Kent Jardemark,** for being my mentor, nice talks, Gothenburghumor, and letting me in your lab during "sommarforskarskola".

I cannot show my appreciation more to Dr. **Michel Goiny**, who contributed a ton to this thesis, thank you for being the go-to guy regarding all things lab related during these years. And for being passionately against bureaucracy.

This thesis had not been possible without the help from all present and former members of the Erhardt/Engberg research group, that being said, big thanks to:

Funda Orhan, for always being sweet, kind, and helpful, and for putting up with all my annoyances, and lack of soul. My apologies for all insults!

Xicong Liu, for your great sense of humor, all strange chats we´ve had thanks to language barriers, and most of all, for telling me everything there is to know about all kinds of rats.

Anthi Faka, for always being encouraging and helpful. And for helping me gain insight into the workings of the female mind. Good luck with everything!

Alexandra Andersson, for being supportive and understanding, and maybe most important of all, for teaching me how to not be needy ☺!

Sophie Imbault, for putting up with endless questions about pronunciation and grammar. Huge thanks also for proof reading and for appreciating (I think) cat videos. There´s no such thing as a "caribou"!!

Magdalena Kegel, who has been a lifesaver, professionally and personally (and being waay too humble about it). Thank you for your generosity and helpfulness. I envy your work capacity.

Klas Linderholm, the MacGyver of the Erhardt/Engberg group. Thanks for being a fellow lover of cute animals and Apple stuff. Huge thanks also for sharing TIPS! regarding almost anything.

Maria Holtze, for always being wise and for saying the stuff that you need to hear but do not want to hear. Thanks also for sharing some of my misanthropic traits.

Sara Olsson, for being a great roommate and for being an awesome human social lubricant. Thank you also for introducing me to loads of stuff as a newbie in the lab.

Maria Fernqvist, and **Maximilian Tufvesson Alm**, for help with paper IV and for being friendly.

Carl Sellgren for invaluable help with statistics and SPSS. **Astra Zeneca** for the grant, making it possible to analyze kynureninemetabolites. **Maria Bhat** for setting up the method analyzing together with **Sara Ståhl**. **Ida Nilsson** for all things staining, imaging and perfusion. **Camilla Svensson** with research group. Alfredo Olivieros, Anna Malmqvist, Dag Holmberg, Ann-Chatrine Samuelsson, Johan Söderlund, Richard Ågren, Oscar Jungholm, Asma Islam.

A big shout-out to past and present doctoral students at FyFa**: Gustaf Wigerblad** and **Carolina Bengtsson-Gonzales** for being great friends and snus-enablers. **Carl Björkholm** for nice chats and trivia. **Åsa Konradsson-Geuken** for awesomeness. **Anna Persson** for nice talks. **Stealth Lars a.k.a Real Bash** for being hilarious while under the influence…Thank you also **Monica Marcus**, **Björn Schilström**, **Torun Malmlöf**, **Anja Finn**.

Thanks to the staff at the department of physiology and pharmacology, especially: **Stefan Eriksson**, **Eva Gipperth**, **Camilla Fors-Holmberg**, **Ylva Haraldsdotter**. **Freddie Hellström**, **Sarah Lindholm**, **Monica Pace-Sjöberg**, **Ulla Wester**, **Renee Andersson**, **Renee Rizzo**, **Inger Johansson**, **Micke Elm** for invaluable help with almost anything. Thanks also to the staff at the animal department, especially **P-A**, **Martina**, and **Josefin**.

Thank you, Dr. **Mats Humble,** for making me interested in neuroscience and helping me getting in touch with the Erhardt/Engberg lab.

Thank you, **Rita Gustafson,** for legal advice and nice whatsapp chats

Thanks to my dear friends from the biomedicine program: **Alex Sångberg, Jacob Kjell**, **My Björkholm**, **Daniella Johansson**, **Mikael Kallin**, **Marie Koitsalu**, **Elina Eriksson**, **Peter Sahlström**, **Jeanette Roos**, **Emma Svedin**, **Tomas Hägglöf, Henning Fernström**.

Thanks to my friends: **Adil Hussain**, **Daniel Kratt**, **Jimmy Nordström**, **Peter Qvist**, **Poojan Ravandoust**.

Thanks to the lovely and awesome Lindkvist/Uihero family, **Annika, Johanna, Ari, Elisabeth** (and **Tomas ☺), Tommy**.

Thank you, **Åsa Glifberg** for being supportive, kind-hearted, and wonderful ❤

Thank you, dear uncle Dr. **Conny Larsson,** and amazing cousins **Emil** and **Johan**, for all your support throughout the years.

Thank you my beloved and sweet sister **Nina Larsson**, for **everything!** Thank you also **Olof** for being wise and supporting, and always making me feel welcome in Malmö! Thank you also of course **Majken** and **Bruno.**

Thank you, **farmor**, for your unconditional love. This thesis is for you!

Thank you **mamma (and Roger)** and **pappa**, for giving me the best upbringing ever, and for always being encouraging and supportive throughout my upbringing.

7 REFERENCES

Abi-Dargham, A., Gil, R., Krystal, J., Baldwin, R.M., Seibyl, J.P., Bowers, M., van Dyck, C.H., Charney, D.S., Innis, R.B., Laruelle, M., 1998. Increased striatal dopamine transmission in schizophrenia: confirmation in a second cohort. Am J Psychiatry 155, 761–767.

Abi-Dargham, A., Laruelle, M., 2005. Mechanisms of action of second generation antipsychotic drugs in schizophrenia: insights from brain imaging studies. Eur. Psychiatry 20, 15–27.

Abi-Dargham, A., Rodenhiser, J., Printz, D., Zea-Ponce, Y., Gil, R., Kegeles, L.S., Weiss, R., Cooper, T.B., Mann, J.J., Van Heertum, R.L., Gorman, J.M., Laruelle, M., 2000. Increased baseline occupancy of D2 receptors by dopamine in schizophrenia. Proc. Natl. Acad. Sci. U.S.A. 97, 8104–8109.

Alexander, K.S., Wu, H.-Q., Schwarcz, R., Bruno, J.P., 2012. Acute elevations of brain kynurenic acid impair cognitive flexibility: normalization by the alpha7 positive modulator galantamine. Psychopharmacology 220, 627–637.

Allen, R.M., Young, S.J., 1978. Phencyclidine-induced psychosis. Am J Psychiatry 135, 1081–1084.

Andreasen, N.C., Olsen, S., 1982. Negative v positive schizophrenia. Definition and validation. Arch. Gen. Psychiatry 39, 789–794.

Araque, A., Parpura, V., Sanzgiri, R.P., Haydon, P.G., 1999. Tripartite synapses: glia, the unacknowledged partner. Trends Neurosci. 22, 208–215.

Asp, L., Beraki, S., Kristensson, K., Ogren, S.O., Karlsson, H., 2009. Neonatal infection with neurotropic influenza A virus affects working memory and expression of type III Nrg1 in adult mice. Brain Behav. Immun. 23, 733–741.

Asp, L., Holtze, M., Powell, S.B., Karlsson, H., Erhardt, S., 2010. Neonatal infection with neurotropic influenza A virus induces the kynurenine pathway in early life and disrupts sensorimotor gating in adult Tap1-/- mice. Int. J. Neuropsychopharm. 13, 475–485.

Bakshi, V.P., Swerdlow, N.R., Geyer, M.A., 1994. Clozapine antagonizes phencyclidine-induced deficits in sensorimotor gating of the startle response. J. Pharmacol. Exp. Ther. 271, 787–794.

Banks, W.A., Robinson, S.M., 2010. Minimal penetration of lipopolysaccharide across the murine blood-brain barrier. Brain Behav. Immun. 24, 102–109.

Baron, M., Gruen, R., 1988. Risk factors in schizophrenia. Season of birth and family history. Br J Psychiatry 152, 460–465.

Bergen, S.E., O'Dushlaine, C.T., Ripke, S., Lee, P.H., Ruderfer, D.M., Akterin, S., Moran, J.L., Chambert, K.D., Handsaker, R.E., Backlund, L., Osby, U., McCarroll, S., Landén, M., Scolnick, E.M., Magnusson, P.K.E., Lichtenstein, P., Hultman, C.M., Purcell, S.M., Sklar, P., Sullivan, P.F., 2012. Genome-wide association study in a Swedish population yields support for greater CNV and MHC involvement in schizophrenia compared with bipolar disorder. Mol. Psychiatry 17, 880–886.

Bleuler, E., 1911. Dementia praecox, oder Gruppe der Schizophrenien. Leipzig: Deuticke.

Braff, D., Stone, C., Callaway, E., Geyer, M.A., Glick, I., Bali, L., 1978. Prestimulus effects on human startle reflex in normals and schizophrenics. Psychophysiology 15, 339–343.

Breier, A., Malhotra, A.K., Pinals, D.A., Weisenfeld, N.I., Pickar, D., 1997a. Association of ketamine-induced psychosis with focal activation of the prefrontal cortex in healthy volunteers. Am J Psychiatry 154, 805–811.

Breier, A., Su, T.P., Saunders, R., Carson, R.E., Kolachana, B.S., de Bartolomeis, A., Weinberger, D.R., Weisenfeld, N., Malhotra, A.K., Eckelman, W.C., Pickar, D., 1997b. Schizophrenia is associated with elevated amphetamine-induced synaptic dopamine concentrations: evidence from a novel positron emission tomography method. Proc. Natl. Acad. Sci. U.S.A. 94, 2569–2574.

Brooks, J.M., Pershing, M.L., Thomsen, M.S., Mikkelsen, J.D., Sarter, M., Bruno, J.P., 2012. Transient Inactivation of the Neonatal Ventral Hippocampus Impairs Attentional Set-Shifting Behavior: Reversal with an α7 Nicotinic Agonist. Neuropsychopharmacology 37, 2476–2486.

Brown, A.S., Hooton, J., Schaefer, C.A., Zhang, H., Petkova, E., Babulas, V., Perrin, M., Gorman, J.M., Susser, E.S., 2004. Elevated maternal interleukin-8 levels and risk of schizophrenia in adult offspring. Am J Psychiatry 161, 889–895.

Bychkov, E.R., Ahmed, M.R., Gurevich, V.V., Benovic, J.L., Gurevich, E.V., 2011. Reduced expression of G protein-coupled receptor kinases in schizophrenia but not in schizoaffective disorder. Neurobiol. Dis. 44, 248–258.

Campbell, B.M., Charych, E., Lee, A.W., Möller, T., 2014. Kynurenines in CNS disease: regulation by inflammatory cytokines. Front Neurosci 8, 12.

Cannon, T.D., Kaprio, J., Lönnqvist, J., Huttunen, M., Koskenvuo, M., 1998. The genetic epidemiology of schizophrenia in a Finnish twin cohort. A population-based modeling study. Arch. Gen. Psychiatry 55, 67–74.

Cardno, A.G., Gottesman, I.I., 2000. Twin studies of schizophrenia: from bow-and-arrow concordances to star wars Mx and functional genomics. Am. J. Med. Genet. 97, 12–17.

Cardno, A.G., Marshall, E.J., Coid, B., Macdonald, A.M., Ribchester, T.R., Davies, N.J., Venturi, P., Jones, L.A., Lewis, S.W., Sham, P.C., Gottesman, I.I., Farmer, A.E., McGuffin, P., Reveley, A.M., Murray, R.M., 1999. Heritability estimates for psychotic disorders: the Maudsley twin psychosis series. Arch. Gen. Psychiatry 56, 162–168.

Carlsson, A., Waters, N., Holm-Waters, S., Tedroff, J., Nilsson, M., Carlsson, M.L., 2001. Interactions between monoamines, glutamate, and GABA in schizophrenia: new evidence. Annu. Rev. Pharmacol. Toxicol. 41, 237–260.

Czerniawski, J., Miyashita, T., Lewandowski, G., Guzowski, J.F., 2015. Systemic lipopolysaccharide administration impairs retrieval of context-object discrimination, but not spatial, memory: Evidence for selective disruption of specific hippocampus-dependent memory functions during acute neuroinflammation. Brain Behav. Immun. 44, 159–166.

Davis, K.L., Kahn, R.S., Ko, G., Davidson, M., 1991. Dopamine in schizophrenia: a review and reconceptualization. Am J Psychiatry 148, 1474–1486.

de Vries, H.E., Moor, A.C., Blom-Roosemalen, M.C., de Boer, A.G., Breimer, D.D., van Berkel, T.J., Kuiper, J., 1994. Lymphocyte adhesion to brain capillary endothelial cells in vitro. J. Neuroimmunol. 52, 1–8.

Desai, P.R., Lawson, K.A., Barner, J.C., 2013. Estimating the direct and indirect costs for community-dwelling patients with schizophrenia. JPHSR 4, 187–194.

DiNatale, B.C., Murray, I.A., Schroeder, J.C., Flaveny, C.A., Lahoti, T.S., Laurenzana, E.M., Omiecinski, C.J., Perdew, G.H., 2010. Kynurenic acid is a potent endogenous aryl hydrocarbon receptor ligand that synergistically induces interleukin-6 in the presence of inflammatory signaling. Toxicol. Sci. 115, 89–97.

Dong, Y., Benveniste, E.N., 2001. Immune function of astrocytes. Glia 36, 180–190.
Doorduin, J., de Vries, E.F.J., Willemsen, A.T.M., de Groot, J.C., Dierckx, R.A., Klein, H.C., 2009. Neuroinflammation in schizophrenia-related psychosis: a PET study. J. Nucl. Med. 50, 1801–1807.
Dunn, A., Swiergiel, A., 2005. Effects of interleukin-1 and endotoxin in the forced swim and tail suspension tests in mice. Pharmacology Biochemistry and Behavior 81, 688–693.
Eltzschig, H.K., Sitkovsky, M.V., Robson, S.C., 2012. Purinergic Signaling during Inflammation. N. Engl. J. Med. 367, 2322–2333.
Erhardt, S., Blennow, K., Nordin, C., Skogh, E., Lindström, L.H., Engberg, G., 2001a. Kynurenic acid levels are elevated in the cerebrospinal fluid of patients with schizophrenia. Neurosci. Lett. 313, 96–98.
Erhardt, S., Oberg, H., Mathé, J.M., Engberg, G., 2001b. Pharmacological elevation of endogenous kynurenic acid levels activates nigral dopamine neurons. Amino Acids 20, 353–362.
Erhardt, S., Schwieler, L., Emanuelsson, C., Geyer, M.A., 2004. Endogenous kynurenic acid disrupts prepulse inhibition. Biol. Psychiatry 56, 255–260.
Falsig, J., van Beek, J., Hermann, C., Leist, M., 2008. Molecular basis for detection of invading pathogens in the brain. J. Neurosci. Res. 86, 1434–1447.
Feng, Y.-H., Wang, L., Wang, Q., Li, X., Zeng, R., Gorodeski, G.I., 2005. ATP stimulates GRK-3 phosphorylation and beta-arrestin-2-dependent internalization of P2X7 receptor. Am. J. Physiol., Cell Physiol. 288, C1342–56.
Fields, R.D., Burnstock, G., 2006. Purinergic signalling in neuron-glia interactions. Nat. Rev. Neurosci. 7, 423–436. doi:10.1038/nrn1928
Fijał, K., Popik, P., Nikiforuk, A., 2014. Co-administration of 5-HT6 receptor antagonists with clozapine, risperidone, and a 5-HT2A receptor antagonist: effects on prepulse inhibition in rats. Psychopharmacology 231, 269–281.
Gál, E.M., Sherman, A.D., 1980. L-Kynurenine - Its Synthesis and Possible Regulatory Function in Brain. Neurochem. Res. 5, 223–239.
Geyer, M.A., Krebs-Thomson, K., Braff, D.L., Swerdlow, N.R., 2001. Pharmacological studies of prepulse inhibition models of sensorimotor gating deficits in schizophrenia: a decade in review. Psychopharmacology 156, 117–154.
Goshen, I., Kreisel, T., Ounallah-Saad, H., Renbaum, P., Zalzstein, Y., Ben-Hur, T., Levy-Lahad, E., Yirmiya, R., 2007. A dual role for interleukin-1 in hippocampal-dependent memory processes. Psychoneuroendocrinology 32, 1106–1115.
Gresack, J.E., Risbrough, V.B., 2011. Corticotropin-releasing factor and noradrenergic signalling exert reciprocal control over startle reactivity. Int. J. Neuropsychopharmacol. 14, 1179–1194.
Gupta, R., Assalman, I., Bottlender, R., 2012. Menopause and schizophrenia. Menopause Int 18, 10–14.
Haba, R., Shintani, N., Onaka, Y., Wang, H., Takenaga, R., Hayata, A., Baba, A., Hashimoto, H., 2012. Lipopolysaccharide affects exploratory behaviors toward novel objects by impairing cognition and/or motivation in mice: Possible role of activation of the central amygdala. Behav. Brain Res. 228, 423–431.
Hart, B.L., 1988. Biological Basis of the Behavior of Sick Animals. Neurosci Biobehav Rev 12, 123–137.
Hilmas, C., Pereira, E.F., Alkondon, M., Rassoulpour, A., Schwarcz, R., Albuquerque, E.X., 2001. The brain metabolite kynurenic acid inhibits alpha7 nicotinic receptor activity and increases non-alpha7 nicotinic receptor expression: physiopathological implications. J. Neurosci. 21, 7463–7473.

Jakobsson, J., Stridsberg, M., Zetterberg, H., Blennow, K., Ekman, C.J., Johansson, A.G.M., Sellgren, C., Landén, M., 2013. Decreased cerebrospinal fluid secretogranin II concentrations in severe forms of bipolar disorder. J Psychiatry Neurosci 38, E21–6.
Jangula, A., Murphy, E.J., 2013. Lipopolysaccharide-induced blood brain barrier permeability is enhanced by alpha-synuclein expression. Neurosci. Lett. 551, 23–27.
Jauregg, von, J.W., 1926. Fieberbehandlung bei psychosen. Wien Med Wochenschr.
Jiang, L.-H., Baldwin, J.M., Roger, S., Baldwin, S.A., 2013. Insights into the Molecular Mechanisms Underlying Mammalian P2X7 Receptor Functions and Contributions in Diseases, Revealed by Structural Modeling and Single Nucleotide Polymorphisms. Front Pharmacol 4, 55.
Josefsson, M., Roman, M., Skogh, E., Dahl, M.-L., 2010. Liquid chromatography/tandem mass spectrometry method for determination of olanzapine and N-desmethylolanzapine in human serum and cerebrospinal fluid. J Pharm Biomed Anal 53, 576–582.
Kim, J.S., Kornhuber, H.H., Schmid-Burgk, W., Holzmüller, B., 1980. Low cerebrospinal fluid glutamate in schizophrenic patients and a new hypothesis on schizophrenia. Neurosci. Lett. 20, 379–382.
Kozak, R., Campbell, B.M., Strick, C.A., Horner, W., Hoffmann, W.E., Kiss, T., Chapin, D.S., McGinnis, D., Abbott, A.L., Roberts, B.M., Fonseca, K., Guanowsky, V., Young, D.A., Seymour, P.A., Dounay, A., Hajos, M., Williams, G.V., Castner, S.A., 2014. Reduction of brain kynurenic Acid improves cognitive function. J. Neurosci. 34, 10592–10602.
Kraepelin, E., 1896. Lehrbuch der psychiatrie. Leipzig: Barth.
Krystal, J.H., Perry, E.B., Gueorguieva, R., Belger, A., Madonick, S.H., Abi-Dargham, A., Cooper, T.B., Macdougall, L., Abi-Saab, W., D'Souza, D.C., 2005. Comparative and interactive human psychopharmacologic effects of ketamine and amphetamine: implications for glutamatergic and dopaminergic model psychoses and cognitive function. Arch. Gen. Psychiatry 62, 985–994.
Lahti, A.C., Weiler, M.A., Tamara Michaelidis, B.A., Parwani, A., Tamminga, C.A., 2001. Effects of ketamine in normal and schizophrenic volunteers. Neuropsychopharmacology 25, 455–467.
Lapin, I.P., 1978. Stimulant and convulsive effects of kynurenines injected into brain ventricles in mice. J Neural Transm 42, 37–43.
Laruelle, M., Abi-Dargham, A., van Dyck, C.H., Gil, R., D'Souza, C.D., Erdos, J., McCance, E., Rosenblatt, W., Fingado, C., Zoghbi, S.S., Baldwin, R.M., Seibyl, J.P., Krystal, J.H., Charney, D.S., Innis, R.B., 1996. Single photon emission computerized tomography imaging of amphetamine-induced dopamine release in drug-free schizophrenic subjects. Proc. Natl. Acad. Sci. U.S.A. 93, 9235–9240.
Levkovitz, Y., Mendlovich, S., Riwkes, S., Braw, Y., Levkovitch-Verbin, H., Gal, G., Fennig, S., Treves, I., Kron, S., 2010. A double-blind, randomized study of minocycline for the treatment of negative and cognitive symptoms in early-phase schizophrenia. J Clin Psychiatry 71, 138–149.
Li, M., He, E., Volf, N., 2011. Time course of the attenuation effect of repeated antipsychotic treatment on prepulse inhibition disruption induced by repeated phencyclidine treatment. Pharmacol. Biochem. Behav. 98, 559–569.
Liebig, J., 1853. Uber Kynurensäure. Justus Liebigs Ann. Chem 125–126.
Lim, A.L., Taylor, D.A., Malone, D.T., 2012. Consequences of early life MK-801 administration: long-term behavioural effects and relevance to schizophrenia research. Behav. Brain Res. 227, 276–286.

Linderholm, K.R., Andersson, A., Olsson, S.K., Olsson, E., Snodgrass, R., Engberg, G., Erhardt, S., 2007. Activation of rat ventral tegmental area dopamine neurons by endogenous kynurenic acid: a pharmacological analysis. Neuropharmacology 53, 918–924.
Linderholm, K.R., Skogh, E., Olsson, S.K., Dahl, M.-L., Holtze, M., Engberg, G., Samuelsson, M., Erhardt, S., 2012. Increased levels of kynurenine and kynurenic acid in the CSF of patients with schizophrenia. Schizophr Bull 38, 426–432.
Lipina, T.V., Roder, J.C., 2014. Disrupted-In-Schizophrenia-1 (DISC1) interactome and mental disorders: impact of mouse models. Neurosci Biobehav Rev 45, 271–294.
Lipska, B.K., Weinberger, D.R., 2002. A neurodevelopmental model of schizophrenia: neonatal disconnection of the hippocampus. Neurotox Res 4, 469–475.
Liu, F., Guo, X., Wu, R., Ou, J., Zheng, Y., Zhang, B., Xie, L., Zhang, L., Yang, L., Yang, S., Yang, J., Ruan, Y., Zeng, Y., Xu, X., Zhao, J., 2014. Minocycline supplementation for treatment of negative symptoms in early-phase schizophrenia: a double blind, randomized, controlled trial. Schizophr. Res. 153, 169–176.
Liu, X.C., Holtze, M., Powell, S.B., Terrando, N., Larsson, M.K., Persson, A., Olsson, S.K., Orhan, F., Kegel, M.E., Asp, L., Goiny, M., Schwieler, L., Engberg, G., Karlsson, H., Erhardt, S., 2014. Behavioral disturbances in adult mice following neonatal virus infection or kynurenine treatment – role of brain kynurenic acid. Brain Behav. Immun. 36, 80–89.
Malhotra, A.K., Adler, C.M., Kennison, S.D., Elman, I., Pickar, D., Breier, A., 1997. Clozapine blunts N-methyl-D-aspartate antagonist-induced psychosis: a study with ketamine. Biol. Psychiatry 42, 664–668.
Martinon, F., Gaide, O., Pétrilli, V., Mayor, A., Tschopp, J., 2007. NALP inflammasomes: a central role in innate immunity. Semin Immunopathol 29, 213–229.
McGhie, A., Chapman, J., 1961. Disorders of attention and perception in early schizophrenia. Br J Med Psychol 34, 103–116.
McGrath, J., Saha, S., Chant, D., Welham, J., 2008. Schizophrenia: a concise overview of incidence, prevalence, and mortality. Epidemiol Rev 30, 67–76.
McGrath, J., Saha, S., Welham, J., Saadi, El, O., MacCauley, C., Chant, D., 2004. A systematic review of the incidence of schizophrenia: the distribution of rates and the influence of sex, urbanicity, migrant status and methodology. BMC Med 2, 13.
Mellergard, M., 1980. Schizophrenia - an International Follow-Up-Study - Who. Acta Psychiatr Scand 61, 486–487.
Menninger, K.A., 1919. Psychoses Associated with Influenza. I. A Statistical Analysis. Jour. Am. Med. Assn.
Miller, B.J., Buckley, P., Seabolt, W., Mellor, A., Kirkpatrick, B., 2011. Meta-analysis of cytokine alterations in schizophrenia: clinical status and antipsychotic effects. Biol. Psychiatry 70, 663–671.
Ming, Z., Sawicki, G., Bekar, L.K., 2015. Acute systemic LPS-mediated inflammation induces lasting changes in mouse cortical neuromodulation and behavior. Neurosci. Lett. 590, 96–100.
Minkiewicz, J., de Rivero Vaccari, J.P., Keane, R.W., 2013. Human astrocytes express a novel NLRP2 inflammasome. Glia 61, 1113–1121.
Moroni, F., Cozzi, A., Carpendo, R., Cipriani, G., Veneroni, O., Izzo, E., 2005. Kynurenine 3-mono-oxygenase inhibitors reduce glutamate concentration in the extracellular spaces of the basal ganglia but not in those of the cortex or hippocampus. Neuropharmacology 48, 788–795.
Moroni, F., Russi, P., Lombardi, G., Beni, M., Carlà, V., 1988. Presence of kynurenic acid in the mammalian brain. J. Neurochem. 51, 177–180.

Muraki, K., Tanigaki, K., 2015. Neuronal migration abnormalities and its possible implications for schizophrenia. Front Neurosci 9, 74.
Müller, N., Riedel, M., Schwarz, M.J., Engel, R.R., 2005. Clinical effects of COX-2 inhibitors on cognition in schizophrenia. Eur Arch Psychiatry Clin Neurosci 255, 149–151.
Nilsson, L.K., Linderholm, K.R., Engberg, G., Paulson, L., Blennow, K., Lindström, L.H., Nordin, C., Karanti, A., Persson, P., Erhardt, S., 2005. Elevated levels of kynurenic acid in the cerebrospinal fluid of male patients with schizophrenia. Schizophr. Res. 80, 315–322.
Nimmerjahn, A., Kirchhoff, F., Helmchen, F., 2005. Resting microglial cells are highly dynamic surveillants of brain parenchyma in vivo. Science 308, 1314–1318.
O'Connor, J.C., Lawson, M.A., Andre, C., Moreau, M., Lestage, J., Castanon, N., Kelley, K.W., Dantzer, R., 2009. Lipopolysaccharide-induced depressive-like behavior is mediated by indoleamine 2,3-dioxygenase activation in mice. Mol. Psychiatry 14, 511–522.
Olsson, S.K., Andersson, A.S., Linderholm, K.R., Holtze, M., Nilsson-Todd, L.K., Schwieler, L., Olsson, E., Larsson, K., Engberg, G., Erhardt, S., 2009. Elevated levels of kynurenic acid change the dopaminergic response to amphetamine: implications for schizophrenia. Int. J. Neuropsychopharmacol. 12, 501–512.
Olsson, S.K., Sellgren, C., Engberg, G., Landén, M., Erhardt, S., 2012. Cerebrospinal fluid kynurenic acid is associated with manic and psychotic features in patients with bipolar I disorder. Bipolar Disord 14, 719–726.
Paxinos, G., Franklin, K.B.J., 2008. The Mouse Brain in Stereotaxic Coordinates. Academic Press.
Peppel, K., Boekhoff, I., McDonald, P., Breer, H., Caron, M.G., Lefkowitz, R.J., 1997. G protein-coupled receptor kinase 3 (GRK3) gene disruption leads to loss of odorant receptor desensitization. J. Biol. Chem. 272, 25425–25428.
Persidsky, Y., Stins, M., Way, D., Witte, M.H., Weinand, M., Kim, K.S., Bock, P., Gendelman, H.E., Fiala, M., 1997. A model for monocyte migration through the blood-brain barrier during HIV-1 encephalitis. J. Immunol. 158, 3499–3510.
Potter, M.C., Elmer, G.I., Bergeron, R., Albuquerque, E.X., Guidetti, P., Wu, H.-Q., Schwarcz, R., 2010. Reduction of endogenous kynurenic acid formation enhances extracellular glutamate, hippocampal plasticity, and cognitive behavior. Neuropsychopharmacology 35, 1734–1742.
Powell, S.B., Zhou, X., Geyer, M.A., 2009. Prepulse inhibition and genetic mouse models of schizophrenia. Behav. Brain Res. 204, 282–294.
Rao, J.S., Rapoport, S.I., Kim, H.-W., 2009. Decreased GRK3 but not GRK2 expression in frontal cortex from bipolar disorder patients. Int. J. Neuropsychopharmacol. 12, 851–860.
Reiprich, P., 2004. Neonatal NMDA Receptor Blockade Disturbs Neuronal Migration in Rat Somatosensory Cortex In Vivo. Cerebral Cortex 15, 349–358.
Reyes, T.M., Fabry, Z., Coe, C.L., 1999. Brain endothelial cell production of a neuroprotective cytokine, interleukin-6, in response to noxious stimuli. Brain Res. 851, 215–220.
Rhee, S.H., Hwang, D., 2000. Murine TOLL-like receptor 4 confers lipopolysaccharide responsiveness as determined by activation of NF kappa B and expression of the inducible cyclooxygenase. J. Biol. Chem. 275, 34035–34040.
Saha, S., Chant, D., McGrath, J., 2007. A Systematic Review of Mortality in Schizophrenia: Is the Differential Mortality Gap Worsening Over Time? Arch. Gen. Psychiatry 64, 1123–1131.

Salazar, A., Gonzalez-Rivera, B.L., Redus, L., Parrott, J.M., O'Connor, J.C., 2012. Indoleamine 2,3-dioxygenase mediates anhedonia and anxiety-like behaviors caused by peripheral lipopolysaccharide immune challenge. Horm Behav 62, 202–209.
Sanfilipo, M., Wolkin, A., Angrist, B., van Kammen, D.P., Duncan, E., Wieland, S., Cooper, T.B., Peselow, E.D., Rotrosen, J., 1996. Amphetamine and negative symptoms of schizophrenia. Psychopharmacology 123, 211–214.
Sanz, J.M., Di Virgilio, F., 2000. Kinetics and mechanism of ATP-dependent IL-1 beta release from microglial cells. J. Immunol. 164, 4893–4898.
Sathyasaikumar, K.V., Stachowski, E.K., Wonodi, I., Roberts, R.C., Rassoulpour, A., McMahon, R.P., Schwarcz, R., 2011. Impaired kynurenine pathway metabolism in the prefrontal cortex of individuals with schizophrenia. Schizophr Bull 37, 1147–1156.
Schwarcz, R., Rassoulpour, A., Wu, H.Q., Medoff, D., Tamminga, C.A., Roberts, R.C., 2001. Increased cortical kynurenate content in schizophrenia. Biol. Psychiatry 50, 521–530.
Schwarcz, R., Whetsell, W.O., Mangano, R.M., 1983. Quinolinic Acid - an Endogenous Metabolite That Produces Axon-Sparing Lesions in Rat-Brain. Science 219, 316–318.
Sellgren, C., Kegel, M.E., Kegel, M.E., Bergen, S.E., Ekman, C.J., Olsson, S.K., Larsson, M.K., Vawter, M.P., Schalling, M., Backlund, L., Sullivan, P.F., Sklar, P., Smoller, J.W., Magnusson, P.K.E., Hultman, C.M., Walther-Jallow, L., Svensson, C.I., Lichtenstein, P., Engberg, G., Erhardt, S., Landén, M., 2015. An inflammatory pathway linked to psychosis in bipolar disorder. Submitted.
Semple, D.M., McIntosh, A.M., Lawrie, S.M., 2005. Cannabis as a risk factor for psychosis: systematic review. Journal of Psychopharmacology 19, 187–194.
Shaltiel, G., Shamir, A., Levi, I., Bersudsky, Y., Agam, G., 2006. Lymphocyte G-protein receptor kinase (GRK)3 mRNA levels in bipolar disorder. Int. J. Neuropsychopharm. 9, 761–766.
Shi, J., Levinson, D.F., Duan, J., Sanders, A.R., Zheng, Y., Pe'er, I., Dudbridge, F., Holmans, P.A., Whittemore, A.S., Mowry, B.J., Olincy, A., Amin, F., Cloninger, C.R., Silverman, J.M., Buccola, N.G., Byerley, W.F., Black, D.W., Crowe, R.R., Oksenberg, J.R., Mirel, D.B., Kendler, K.S., Freedman, R., Gejman, P.V., 2009. Common variants on chromosome 6p22.1 are associated with schizophrenia. Nature 460, 753–757.
Skogh, E., Sjödin, I., Josefsson, M., Dahl, M.-L., 2011. High correlation between serum and cerebrospinal fluid olanzapine concentrations in patients with schizophrenia or schizoaffective disorder medicating with oral olanzapine as the only antipsychotic drug. J Clin Psychopharmacol 31, 4–9.
Snyder, S.H., 1973. Amphetamine psychosis: a “model” schizophrenia mediated by catecholamines. Am J Psychiatry 130, 61–67.
Söderlund, J., Schröder, J., Nordin, C., Samuelsson, M., Walther-Jallow, L., Karlsson, H., Erhardt, S., Engberg, G., 2009. Activation of brain interleukin-1beta in schizophrenia. Mol. Psychiatry 14, 1069–1071.
Sperlágh, B., Illes, P., 2014. P2X7 receptor: an emerging target in central nervous system diseases. Trends in Pharmacological Sciences 35, 537–547.
Stafford, M.R., Jackson, H., Mayo-Wilson, E., Morrison, A.P., Kendall, T., 2013. Early interventions to prevent psychosis: systematic review and meta-analysis. BMJ 346, f185–f185.
Stone, T.W., Perkins, M.N., 1981. Quinolinic acid: a potent endogenous excitant at amino acid receptors in CNS. Eur. J. Pharmacol. 72, 411–412.
Sullivan, P.F., Kendler, K.S., Neale, M.C., 2003. Schizophrenia as a complex trait: evidence from a meta-analysis of twin studies. Arch. Gen. Psychiatry 60, 1187–1192.

Swartz, K.J., During, M.J., Freese, A., Bear, M.F., 1990. Cerebral synthesis and release of kynurenic acid: an endogenous antagonist of excitatory amino acid receptors. J. Neurosci. 10, 2965–2973.
Swerdlow, N.R., Weber, M., Qu, Y., Light, G.A., Braff, D.L., 2008. Realistic expectations of prepulse inhibition in translational models for schizophrenia research. Psychopharmacology 199, 331–388.
Tamminga, C.A., Buchanan, R.W., Gold, J.M., 1998. The role of negative symptoms and cognitive dysfunction in schizophrenia outcome. International Clinical Psychopharmacology 13, 21–26.
Uwai, Y., Honjo, H., Iwamoto, K., 2012. Interaction and transport of kynurenic acid via human organic anion transporters hOAT1 and hOAT3. Pharmacological Research 65, 254–260.
van Berckel, B.N., Bossong, M.G., Boellaard, R., Kloet, R., Schuitemaker, A., Caspers, E., Luurtsema, G., Windhorst, A.D., Cahn, W., Lammertsma, A.A., Kahn, R.S., 2008. Microglia activation in recent-onset schizophrenia: a quantitative (R)-[11C]PK11195 positron emission tomography study. Biol. Psychiatry 64, 820–822.
Vinkers, C.H., Risbrough, V.B., Geyer, M.A., Caldwell, S., Low, M.J., Hauger, R.L., 2007. Role of dopamine D1 and D2 receptors in CRF-induced disruption of sensorimotor gating. Pharmacol. Biochem. Behav. 86, 550–558.
Walker, A.K., Budac, D.P., Bisulco, S., Lee, A.W., Smith, R.A., Beenders, B., Kelley, K.W., Dantzer, R., 2013. NMDA receptor blockade by ketamine abrogates lipopolysaccharide-induced depressive-like behavior in C57BL/6J mice. Neuropsychopharmacology 38, 1609–1616.
Walz, W., 2000. Role of astrocytes in the clearance of excess extracellular potassium. Neurochemistry International 36, 291–300.
Wang, J., Simonavicius, N., Wu, X., Swaminath, G., Reagan, J., Tian, H., Ling, L., 2006. Kynurenic acid as a ligand for orphan G protein-coupled receptor GPR35. J. Biol. Chem. 281, 22021–22028.
Wonodi, I., Stine, O.C., Sathyasaikumar, K.V., Roberts, R.C., Mitchell, B.D., Hong, L.E., Kajii, Y., Thaker, G.K., Schwarcz, R., 2011. Downregulated kynurenine 3-monooxygenase gene expression and enzyme activity in schizophrenia and genetic association with schizophrenia endophenotypes. Arch. Gen. Psychiatry 68, 665–674.
Yolken, R.H., Torrey, E.F., 2008. Are some cases of psychosis caused by microbial agents? A review of the evidence. Mol. Psychiatry 13, 470–479.
Yung, A.R., McGorry, P.D., 1996. The prodromal phase of first-episode psychosis: past and current conceptualizations. Schizophr Bull 22, 353–370.
Zelante, T., Fallarino, F., Bistoni, F., Puccetti, P., Romani, L., 2009. Indoleamine 2,3-dioxygenase in infection: the paradox of an evasive strategy that benefits the host. Microbes Infect. 11, 133–141.
Zunszain, P.A., Anacker, C., Cattaneo, A., Choudhury, S., Musaelyan, K., Myint, A.M., Thuret, S., Price, J., Pariante, C.M., 2012. Interleukin-1β: a new regulator of the kynurenine pathway affecting human hippocampal neurogenesis. Neuropsychopharmacology 37, 939–949.